A LN cells from primed mice

Y1 receptor

GAPDH

B Spleen T cells from naive mice

Y1 receptor

GAPDH

FIGURE 7. Constitutive expression of Y_1 receptor mRNA in LN cells from immunized animals and T cells from naive mice. A, LN cells from animals immunized with MOG_{35-55} express Y_1 receptor RNA (left panels). LN cells were prepared as described in Material and Methods. RNA from homogenized mouse brain was used as a positive control (right panels in both A and B). One representative experiment is shown. B, T cells isolated from spleens of naive animals also express Y_1 receptor RNA (left panels). Five micrograms of total RNA were used for RT-PCR, and amplified products were analyzed by agarose gel electrophoresis. GAPDH was used as a control for equal loading. The sizes of the PCR products were 334 bp for the Y_1 receptor and 190 bp for GAPDH.

group), and all the recipient mice died before day 18 after cell transfer. However, there was a clear tendency that mice transferred with T cell blasts from D-His[26]-treated mice would survive for a longer period of time (the date of death in an individual mouse: day 14, day 17, day 17, day 17, day 17) compared with those given the T cell blasts from PBS-treated mice (the date of death: day 8, day 11, day 14, day 15, day 15). In addition, the mice transferred with the T cells from [D-His[26]-treated mice showed a reduced clinical score at day 8 compared with the control mice (1.5 ± 0.5 vs 4.5 ± 0.6). These results indicate that NPY Y_1 agonist is effective also for EAE induced in SJL/J mice and that the mechanism of action is to interfere with the process of effector lymphocyte generation.

Discussion

With regard to the bidirectional interaction between the immune and the nervous system, prior studies have indicated that catecholamines released from sympathetic nerve endings regulate Th1 responses and Th1-mediated disease such as EAE. Our study demonstrates that NPY also plays an important role in the regulation of EAE. It has previously been indicated that NPY modu-
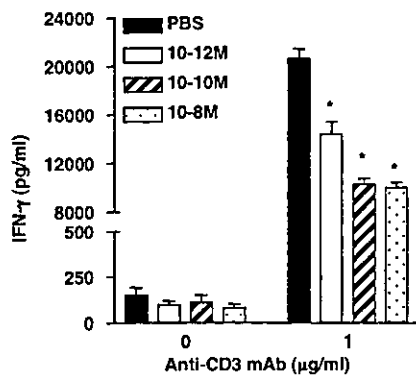

FIGURE 8. Splenocytes from naive mice were stimulated by a plate-bound anti-CD3 mAb in the presence of various concentrations of [D-His[26]]NPY. The Y_1 receptor agonist induced a dose-dependent inhibition of the secretion of IFN-γ in vitro (Y_1 receptor agonist vs control: 10^{-12} M, $p = 0.023$; 10^{-10} M, $p = 0.001$; 10^{-8} M, $p < 0.0001$). Pooled data from three independent experiments are shown ($n = 7$). Error bars, SEM; *, significant differences between treated and untreated conditions.

lates various T cell functions in vitro, including T cell adhesion to integrins (30) and cytokine secretion of in vitro established T clones (22, 23). Our study could be regarded as the first work to provide evidence that NPY modulates T cell function in vivo and that NPY is involved in the natural regulation of Th1-mediated autoimmunity.

The action of NPY is mediated via distinct receptor subtypes such as the Y_1, Y_2, Y_4, and Y_5 receptor. Here we conclude that Y_1 receptors are the main receptor subtypes engaged in the NPY-mediated suppression of EAE. This conclusion was obtained from a series of experiments applying Y_1 receptor agonists and a Y_1 receptor antagonist. Firstly, we showed that the suppressive effect of NPY on EAE was abolished when we coinjected the Y_1 receptor antagonist BIBO3304. Secondly, we replaced native NPY with two types of compounds known to selectively stimulate Y_1 receptors ([D-His[26]]NPY, [F[7],P[34]]NPY) and found that these NPY analogs also effectively suppress the development of EAE. However, a Y_5 receptor agonist was not effective. Thirdly, treatment with BIBO3304 resulted in a significantly earlier onset of disease. All of these results indicate that Y_1 receptor engagement leads to the suppression of EAE.

The Y_1 receptor agonists appear to be much more potent EAE inhibitors than native NPY. In terms of the dosage requirement to gain clinical effects, the hierarchy for the native and altered NPY compounds was apparent ([D-His[26]]NPY > [F[7],P[34]]NPY > native NPY). It seems that the efficacy of these ligands as EAE therapeutics correlates with the specificity for the Y_1 receptors. Namely, [D-His[26]]NPY is more selective for Y_1 receptors, compared with [F[7],P[34]]NPY (24). Taking this into consideration, it is possible that stimulation of non-Y_1 receptors may compete with Y_1 receptor ligation. Alternatively, the Y_1 receptor agonists may be more efficacious as ligands than native NPY in inducing intracellular events leading to the immunoregulation. Alternatively, these differences in the potency of Y_1 receptor compounds and the native peptide NPY may be explained by parallel activation of stimulatory and inhibitory Y receptors by NPY itself rather than by the specific ligands. Furthermore, it is possible that the different Y_1 receptor specific compounds exhibit a differential tissue penetration or may be differentially degraded by specific enzymes such as CD26 (31, 32). Further studies are needed to verify these postulates and provide us with a new insight into NPY-Y_1 receptor interactions.

The experiment using the Y_1 receptor antagonist BIBO3304 showed an earlier onset of EAE, although the disease course was not altered after onset. This indicates that endogenous NPY plays a regulatory role in the induction phase, but not in the effector phase of EAE. Consistent with this, we showed that the treatment during the induction phase is as effective as the continuous treatment covering both induction and effector phases, whereas the treatment starting after onset of EAE does not change the clinical course of EAE. A possible explanation for the failure of the Y_1 receptor antagonist to alter the effector phase is that endogenous NPY levels may substantially decrease in the effector phase, owing to enzymatic degradation. Whereas it is currently impossible to measure the NPY levels in mice with EAE, it is well known that NPY is cleaved by enzymes such as dipeptidyl peptidase IV (CD26), a membrane-bound enzyme, constitutively expressed on numerous cells including leukocytes (31, 32). In addition, activated T cells are reported to express a higher level of CD26 on their surface (33). Thus, it is possible that the contribution of endogenous NPY to the immunoregulation might be reduced in the effector phase because of the rapid degradation by enzymes such as CD26. It is necessary to pursue this issue with different methodologies.

Regarding the mechanism for NPY-mediated suppression of EAE, we showed a significant inhibition of anti-MOG$_{35-55}$ IgG2a titers and of IFN-γ production by MOG$_{35-55}$-specific T cells after treatment with [D-His²⁶]NPY. In contrast, IgG1 titers were unaffected, which resulted in a higher IgG1-IgG2a ratio in treated mice. Also, T cell-proliferative responses were not affected significantly. On the basis of these results, we conclude that NPY plays a selective role in inhibiting IFN-γ production by MOG$_{35-55}$-specific T cells, leading to a Th2 bias. Ex vivo reconstitution experiments also showed that MOG$_{35-55}$-specific T cells are the major target for NPY. Although the presence of functional Y₁ receptors on rat leukocytes has been documented (20, 21), we proved here the presence of mRNA encoding the Y₁ receptor in T cell populations. Accompanying in vitro experiments further confirmed that NPY suppresses T cell production of IFN-γ provoked by CD3 cross-linking.

In conclusion, this study demonstrates for the first time to our knowledge that NPY has an immunomodulatory activity that suppresses signs of EAE. Given that the levels of NPY in the CSF are reduced in patients with MS (34, 35), it is tempting to speculate that NPY may also play a critical role in preventing the development of MS. With the availability of novel and highly selective agonists and their ability to mimic the effects of NPY in a highly specific manner, we propose that targeting NPY receptors may be a promising new therapeutic approach to autoimmune disorders.

Acknowledgments

References

1. Wekerle, H. 1993. Experimental autoimmune encephalomyelitis as a model of immune-mediated CNS disease. *Curr. Opin. Neurobiol. 3:779.*

2. Hemmer, B., S. Cepok, S. Nessler, and N. Sommer. 2002. Pathogenesis of multiple sclerosis: an update on immunology. *Curr. Opin. Neurol. 15:227.*

3. Nicholson, L. B., J. M. Greer, R. A. Sobel, M. B. Lees, and V. K. Kuchroo. 1995. An altered peptide ligand mediates immune deviation and prevents autoimmune encephalomyelitis. *Immunity 3:397.*

4. Aharoni, R., D. Teitelbaum, M. Sela, and R. Arnon. 1997. Copolymer 1 induces T cells of the T helper type 2 that crossreact with myelin basic protein and suppress experimental autoimmune encephalomyelitis. *Proc. Natl. Acad. Sci. USA 94:10821.*

5. Garren, H., P. J. Ruiz, T. A. Watkins, P. Fontoura, L. T. Nguyen, E. R. Estline, D. L. Hirschberg, and L. Steinman. 2001. Combination of gene delivery and DNA vaccination to protection from and reverse Th1 autoimmune disease via deviation to the Th2 pathway. *Immunity 15:15.*

6. Pal, E., T. Tabira, T. Kawano, M. Taniguchi, S. Miyake, and T. Yamamura. 2001. Costimulation-dependent modulation of experimental autoimmune encephalomyelitis by ligand stimulation of Vα14 NK T cells. *J. Immunol. 166:662.*

7. Miyamoto, K., S. Miyake, and T. Yamamura. 2001. A synthetic glycolipid prevents autoimmune encephalomyelitis by inducing TH2 bias of natural killer T cells. *Nature 413:531.*

8. Straub, R. H., J. Westermann, J. Schölmerich, and W. Falk. 1998. Dialogue between the CNS and the immune system in lymphoid organs. *Immunol. Today 19:40.*

9. Elenkov, I. J., R. L. Wilder. G. P. Chrousos, and E. S. Vizi. 2000. The sympathetic nerve: an integrative interface between two supersystems—the brain and the immune system. *Pharmacol. Rev. 52:595.*

10. Downing, J. E., and J. A. Miyan. 2000. Neural immunoregulation: emerging roles for nerves in immune homeostasis and disease. *Immunol. Today 21:281.*

11. Chelmicka-Schorr, E., M. Checineski, and B. G. M. Arnason. 1988. Chemical sympathectomy augments the severity of experimental allergic encephalomyelitis. *J. Neuroimmunol. 17:347.*

12. Chelmicka-Schorr, E., M. N. Kwasniewski, and R. L. Wollmann. 1992. Sympathectomy augments adoptively transferred experimental allergic encephalomyelitis. *J. Neuroimmunol. 37:99.*

13. Chelmicka-Schorr, E., M. N. Kwasniewski, B. E. Thomas, and B. G. Arnason. 1989. The β-adrenergic agonist isoproterenol suppresses experimental allergic encephalomyelitis in Lewis rats. *J. Neuroimmunol. 25:203.*

14. Panina-Bordignon, P., D. Mazzeo, P. D. Lucia, D. D'Ambrosio, R. Lang, L. Fabbri, C. Self, and F. Sinigaglia. 1997. β₂-Agonists prevent Th1 development by selective inhibition of interleukin 12. *J. Clin. Invest. 100:1513.*

15. Kohm, A. P., and V. M. Sanders. 2001. Norepinephrine and β₂-adrenergic receptor stimulation regulate CD4⁺ T and B lymphocyte function in vitro and in vivo. *Pharmacol. Rev. 53:487.*

16. Felten, D. L., S. Y. Felten, S. L. Carlson, J. A. Olshowka, and S. Livnat. 1985. Noradrenergic and peptidergic innervation of lymphoid tissue. *J. Immunol. 135: 755s.*

17. Lundberg, J. M., A. Rudehill, A. Sollevi, G. Fried, and G. Wallin. 1989. Corelease of neuropeptide Y and noradrenaline from pig spleen in vivo: importance of subcellular storage, nerve impulse frequency and pattern, feedback regulation and resupply by axonal transport. *Neuroscience 28:475.*

18. Michel, M. C., A. Beck-Sickinger, H. Cox, H. N. Doods, H. Herzog, D. Larhammar, R. Quirion, T. Schwartz, and T. Westfall. 1998. XVI International Union of Pharmacology recommendations for the nomenclature of neuropeptide Y, peptide YY, and pancreatic polypeptide receptors. *Pharmacol. Rev. 50:143.*

19. Bedoui, S., N. Kawamura, R. H. Straub, R. Pabst, T. Yamamura, and S. von Hörsten. 2003. Relevance of neuropeptide Y for the neuroimmune crosstalk. *J. Neuroimmunol. 134:1.*

20. Petitto, J. M., Z. Huang, and D. B. McCarthy. 1994. Molecular cloning of NPY-Y1 receptor cDNA from rat splenic lymphocytes: evidence of low levels of mRNA expression and [¹²⁵I]-NPY binding sites. *J. Neuroimmunol. 54:81.*

21. Bedoui, S., S. Lechner, T. Gebhardt, H. Nave, A. Beck-Sickinger, R. H. Straub, R. Pabst, and S. von Hörsten. 2002. NPY modulates epinephrine-induced leukocytosis via Y-1 and Y-5 receptor activation in vivo: sympathetic co-transmission during leukocyte mobilization. *J. Neuroimmunol. 132:25.*

22. Kawamura, N., H. Tamura, S. Obana, M. Wenner, T. Ishikawa, A. Nakata, and H. Yamamoto. 1998. Differential effects of neuropeptides on cytokine production by mouse helper T cell subsets. *Neuroimmunomodulation 5:9.*

23. Levite, M. 1998. Neuropeptides, by direct interaction with T cells, induce cytokine secretion and break the commitment to a distinct T helper phenotype. *Proc. Natl. Acad. Sci. USA 95:12544.*

24. Söll, R. M., M. C. Dinger, I. Lundell, D. Larhammar, and A. G. Beck-Sickinger. 2001. Novel analogues of neuropeptide Y with a preference for the Y1-receptor. *Eur. J. Biochem. 268:2828.*

25. Cabrele, C., M. Langer, R. Bader, H. A. Wieland, H. N. Doods, O. Zerbe, and A. G. Beck-Sickinger. 2000. The first selective agonist for the neuropeptide YY5 receptor increases food intake in rats. *J. Biol. Chem. 275:36043.*

26. Mullins, D., D. Kirby, J. Hwa, M. Guzzi, J. Rivier, and E. Parker. 2001. Identification of potent and selective neuropeptide Y Y₁ receptor agonists with orexigenic activity in vivo. *Mol. Pharmacol. 60:534.*

27. Wieland, H. A., W. Engel, W. Eberlein, K. Rudolf, and H. N. Doods. 1998. Subtype selectivity of the novel nonpeptide neuropeptide Y Y₁ receptor antagonist BIBO 3304 and its effect on feeding in rodents. *Br. J. Pharmacol. 125:549.*

28. Avni, O., D. Lee, F. Macian, S. J. Szabo, L. H. Glimcher, and A. Rao. 2002. Th cell differentiation is accompanied by dynamic changes in histone acetylation of cytokine genes. *Nat. Immunol. 3:643.*

29. Bedoui, S., S. Kuhlmann, H. Nave, J. Drube, R. Pabst, and S. von Hörsten. 2001. Differential effects of neuropeptide Y (NPY) on leukocyte subsets in the blood: mobilization of B-1-like B-lymphocytes and activated monocytes. *J. Neuroimmunol. 117:125.*

30. Levite, M., L. Cahalon, R. Hershkoviz, L. Steinman, and O. Lider. 1998. Neuropeptides, via specific receptors, regulate T cell adhesion to fibronectin. *J. Immunol. 160:993.*

31. Fleischer, B. 1994. CD26: a surface protease involved in T-cell activation. *Immunol. Today 15:180.*

32. Mentlein, R. 1999. Dipeptidyl-peptidase IV (CD26): role in the inactivation of regulatory peptides. *Regul. Pept. 85:9.*

33. Gorell, M. D., V. Gysbers, and G. W. McCaughan. 2001. CD26: a multifunctional integral membrane and secreted protein of activated lymphocytes. *Scand. J. Immunol. 54:249.*

34. Maeda, K., M. Yasuda, H. Kaneda, S. Maeda, and A. Yamadori. 1994. Cerebrospinal fluid (CSF) neuropeptide Y- and somatostatin-like immunoreactivities in man. *Neuropeptides 27:323.*

35. Gallai, V., P. Sarchielli, C. Firenze, A. Trequattrini, M. Paciaroni, F. Usai, M. Franceschini, and R. Palumbo. 1994. Neuropeptide Y plasma levels and serum dopamine-beta-hydroxylase activity in MS patients with and without abnormal cardiovascular reflexes. *Acta Neurol. Belg. 94:44.*

Another View of T Cell Antigen Recognition: Cooperative Engagement of Glycolipid Antigens by Va14Ja18 Natural TCR[1]

Aleksandar K. Stanic,* R. Shashidharamurthy,* Jelena S. Bezbradica,* Naoto Matsuki,*
Yoshitaka Yoshimura,* Sachiko Miyake,† Eun Young Choi,‡ Todd D. Schell,§ Luc Van Kaer,*
Satvir S. Tevethia,§ Derry C. Roopenian,‡ Takashi Yamamura,† and Sebastian Joyce[2]*

Va14Ja18 natural T (iNKT) cells rapidly elicit a robust effector response to different glycolipid Ags, with distinct functional outcomes. Biochemical parameters controlling iNKT cell function are partly defined. However, the impact of iNKT cell receptor β-chain repertoire and how α-galactosylceramide (α-GalCer) analogues induce distinct functional responses have remained elusive. Using altered glycolipid ligands, we discovered that the Vb repertoire of iNKT cells impacts recognition and Ag avidity, and that stimulation with suboptimal avidity Ag results in preferential expansion of high-affinity iNKT cells. iNKT cell proliferation and cytokine secretion, which correlate with iNKT cell receptor down-regulation, are induced within narrow biochemical thresholds. Multimers of CD1d1-αGalCer- and αGalCer analogue-loaded complexes demonstrate cooperative engagement of the Va14Ja18 iNKT cell receptor whose structure and/or organization appear distinct from conventional αβ TCR. Our findings demonstrate that iNKT cell functions are controlled by affinity thresholds for glycolipid Ags and reveal a novel property of their Ag receptor apparatus that may have an important role in iNKT cell activation. *The Journal of Immunology*, 2003, 171: 4539–4551.

F undamental to the initiation of a cellular immune response is cell-to-cell communication through receptor triggering and the dynamic formation of an immunological synapse. Central to this process is the interaction between the Ag and its cognate receptor, which relays the specificity of recognition. Although much has been learned regarding the interactions between peptide Ags and their cognate TCR, comparatively little is known about the recognition of CD1-restricted glycolipid Ags by specific T cells.

Va14Ja18 natural T (iNKT)[3] cells are a unique subset of CD1d1-restricted T lymphocytes whose invariant α-chain preferentially pairs with Vb8.2 β-chain and less commonly with Vb7. Remarkably, in vivo iNKT cell activation through the TCR results in rapid (i.e., within 60–90 min) and robust IL-4 response and a spectrum of Th1 and Th2 cytokines (reviewed in Ref. 1). In striking contrast, conventional T lymphocytes require up to a day to produce significant amounts of cytokines in response to Ag.

The natural Ag recognized by iNKT cells remains unknown. A variety of CD1d-positive cells activate freshly isolated thymic iNKT cells and derived hybridomas without the addition of any

exogenous Ag (2–6), which suggests the recognition of self-Ags. Moreover, presentation of self-Ags requires CD1d trafficking through the late endosomes/lysosomes (3, 4, 7–9). The recognition of α-galactosylceramide (αGalCer) and α-glucosylceramide by iNKT cells (10–14) suggests a glycosphingolipid nature of the elusive Ags. Although αGalCer is a nonphysiological Ag, our recent studies indicate that it may be a very close mimic of at least one natural iNKT cell ligand (15). Consistent with this conclusion is the fact that αGalCer and/or its close analogue OCH, with a shortened long-chain sphingosine base and acyl chain, exhibit immunopharmacological effects in vivo. Thus, αGalCer acts like an adjuvant enhancing immunity to malaria and other infectious pathogens (16). Furthermore, αGalCer and/or OCH can prevent autoimmune diseases in mouse models of type I diabetes and multiple sclerosis (17–21). Interestingly, the ability of OCH to induce IL-4 alone and no IFN-γ appears to underlie its pharmacological action (19). Thus, delineating the biochemical parameters of Va14Ja18 TCR/Ag interactions is of paramount pharmacological significance.

Interactions of soluble Ag receptors of conventional T cells with cognate Ags are of low affinity (0.1–50 μM) and relatively fast dissociation half-life ($t_{1/2}$ = 10–50 s) (22–25). Va14Ja18 TCR of an iNKT cell hybridoma has been demonstrated to interact with αGalCer-loaded CD1d1 with relatively high affinity (0.2 μM) and very long half-life ($t_{1/2}$ = 175 s) (26). The high-avidity interaction of Va14Ja18 TCR with CD1d1-αGalCer dimer appears to be influenced by TCR β-chain repertoire (27). Recent studies have implicated both optimal dwell time (28) and affinity (29) of TCR-Ag interaction as critical determinants of T cell sensitivity and activation. Furthermore, interactions of conventional TCR with Ag are thought to be stabilized by CD4 and CD8 coreceptors (30–32). Long dwell time of Va14Ja18 TCR/CD1d1-αGalCer interaction (26) appears counterintuitive to the optimal dwell-time requirements for T cell activation. Because iNKT cells might not use coreceptors during Ag engagement, this interaction might require

intrinsically high affinity and long dwell time for activation of this T cell subset.

Ag recognition by conventional T cells entails self-nonself discrimination. Thus, T cells are tuned to extraordinarily sensitive recognition of foreign Ags (on the order of 20–100 molecules per cell) and base activation decisions on affinity and dwell time (23, 24, 28, 29). Considering that a large body of evidence indicates that iNKT cells recognize self-Ag, a paradox ensues. How is it that iNKT cells are not continually activated by very small amounts of self-Ag presented on APCs in vivo? Self-Ag recognition must be finely tuned to prevent iNKT cell activation during physiological conditions, but to rapidly respond to disturbances in cellular physiology. In other words, iNKT cells need to be very sensitive to modest changes in self-Ag concentration. In biological systems, this kind of fine-tuning is often achieved by cooperative ligand engagement. Cooperativity itself is defined as a positive or negative change in multimeric receptor affinity for ligand following primary and subsequent subunit binding events. Thus, positive cooperativity permits disproportionately sensitive ligand engagement by multimeric receptors, resulting in an almost digital off-on response (33). A form of cooperativity in conventional T cell Ag recognition is afforded by coreceptor-mediated stabilization of TCR-Ag interaction in the immunological synapse. How iNKT cells substitute for coreceptor usage and yet remain unresponsive to low levels of self-Ag remains unknown. Initial report of CD1d1-αGalCer tetramers demonstrated that an iNKT cell hybridoma engages Ag with a Hill coefficient of 4.5, which was interpreted to signify the tetravalency of CD1d1-αGalCer tetramers. Hill coefficient depends on valency but is always lower than the number of binding sites of the multimer (i.e., lower than four for any tetrameric molecule) (34). Because the Hill equation used to calculate the Hill coefficient was not provided in the first (35), how the value of 4.5 was obtained remains elusive.

Several questions regarding CD1d1-lipid/TCR interactions remain: Are there affinity and concentration thresholds for the induction of distinct iNKT cell responses? Does the TCR β-chain repertoire impact iNKT cell Ag reactivity in vivo? Does cooperativity play a role in iNKT cell receptor-Ag interactions? In studies relevant to these questions, we demonstrate that the avidity thresholds for iNKT cell receptor determine sensitivity for glycolipid Ag recognition. Despite the invariant nature of the TCR α-chain, TCR β-chain usage by iNKT cells critically impacts the specificity and the avidity for glycolipid Ags. Furthermore, when responding to a suboptimal affinity ligand, high relative avidity iNKT cells are selected. Interestingly, iNKT cell receptor appears to have structure and/or organization distinct from other αβ TCR and engages Ag cooperatively. Taken together, these features of iNKT cell receptor permit sensitive self-Ag recognition and determine their functional outcomes.

Materials and Methods
Mice

Experiments with B6-Jal8$^{-\prime-}$ (36) (a gift from M. Taniguchi (University of Chiba, Chiba, Japan)), B6.129-CD1d1$^{0/0}$ (37), and C57BL/6 (The Jackson Laboratory, Bar Harbor, ME) were in compliance with the regulations of the Institutional Animal Care and Use Committee of Vanderbilt University.

Cell lines and hybridomas

CTL clones and hybridomas (generously provided by A. Bendelac (Princeton University, Princeton, NJ) and K. Hayakawa (Fox Chase Cancer Center, Philadelphia, PA)) have been described (38–41).

NKT cell enrichment

C57BL/6 thymocytes and splenocytes reacted with anti-CD161-PE were separated with anti-PE magnetic microbeads using an automated sorter (Miltenyi Biotec, Auburn, CA). Samples were typically >95% CD161$^+$.

Antigens

Glycolipids (12, 19) and peptides (38, 39) have been described. Kirin Brewery (Gumma, Japan) generously provided αGalCer. SV40 T Ag-derived epitope IV (VVYDFLKL), H28 (ILENFPRL), and H60 (LTFNYRNL) peptides were synthesized by F-moc chemistry at the Macromolecular Core Facility (Pennsylvania State University).

Generation of multimers

Preparation of CD1d1-glycolipid (15) and H2K^b-peptide tetramers (27, 28) has been described. Dimers of CD1d1 (custom order; BD PharMingen, San Diego, CA) and H2K^b (DimerX; BD PharMingen) are dimeric owing to their fusion to IgG1 H chains. To obviate the potential for artifacts induced by detection mediated via a fluorochrome-conjugated secondary Ab, the dimers were Alexa Fluor 647- or PE-conjugated via Fab specific for the Fc portion of IgG1 (anti-mouse IgG1 Alexa Fluor 647 and PE Zenon kits; Molecular Probes, Eugene, OR). Every batch of tetramer generated was tested for complete loading of αGalCer and its analogues by glycolipid titration loading and testing by reaction with the best characterized iNKT hybridoma N38-2C12.

Flow cytometry

All Abs were from BD PharMingen unless otherwise stated. Tetramer-stained Va14Ja18 iNKT hybridomas (N37-1H5a, Vb8.2Jb2.6; N38-2C12, Vb8.2Jb2.5; N38-3C3, Vb8.2Jb2.2; and DN32.D3, Vb8.2Jb2.4) were also labeled with anti-TCR Cβ-PE (H57-597), NKT cell-enriched thymocytes and splenocytes with anti-NK1.1-PE (PK136), and anti-TCR Cβ-FITC. CTL clones (SV40 epitope IV-specific 2168T as well as minor histocompatibility (mH) Ag-specific SPH60, BH60, and SPH28) reacted with tetramers were also stained with anti-CD8α-FITC. Samples were analyzed using FACSCalibur and CellQuest, version 3.0 (BD Biosciences, Franklin Lakes, NJ) as well as FlowJo 4.2 (Tree Star, San Carlos, CA).

Determination of relative avidity (K_{av})

Equilibrium (>2 h) binding experiments were performed using increasing tetramer concentrations in 100 μl of PBS containing 2% FCS (Invitrogen, Carlsbad, CA) and 0.05% NaN$_3$ at 4°C, to prevent capping and internalization of the TCR. K_{av} was calculated from specific mean fluorescence intensity (MFI; difference between total MFI at a defined tetramer concentration and background MFI derived from ligand-free tetramer binding to the same cells) using nonlinear regression analysis fitted to classical Michaelis-Menten kinetics (Prism 3.02; GraphPad Software, San Diego, CA). MFI (% maximum) shown in the relevant figures is based on V_{max} calculated from nonlinear regression analysis of the data for adequate graphical representation. This permits easy and reliable comparison of data generated in different experiments. Nonlinear Michaelis-Menten regression analysis was preferred, because Scatchard transformation, which uses linear regression, amplifies any variation of the data from the linear curve. That notwithstanding, the results from the Michaelis-Menten kinetics were confirmed by using classical Scatchard transformations to derive the K_{av} (42).

Determination of off-rates

T cells were labeled with 50 μg/ml H2K^b-peptide or 10 μg/ml CD1d-glycolipid tetramers, respectively, incubated at 4°C for 3 h, and washed extensively. Cells were also stained with 10 μg/ml anti-TCR Cβ-FITC to monitor TCR levels. Following initial tetramer binding, 10^6 cells were chased in 3 ml of buffer with rocking at 4 or 37°C for the indicated time periods and analyzed by flow cytometry.

Measurement of in vivo and in vitro cytokine response

Mice were injected i.v. with the indicated concentrations of glycolipids diluted in PBS from a 220 μg/ml stock solution in vehicle (0.5% v/v polysorbate and 0.9% w/v NaCl). Controls were injected with corresponding dose of vehicle. After 90 min, IL-2, IL-4, IL-13, CSF-2, IFN-γ, and TNF-α in control and immune sera were measured by ELISA using Abs and methods that we have described previously (43).

TCR down-regulation and in vitro expansion

Bulk C57BL/6 splenocytes were incubated for the indicated amounts of time with increasing concentrations of glycolipid Ags. Following stimulation, iNKT cell receptor level was determined by flow-cytometric analysis

following staining with CD1d1-αGalCer tetramer, anti-TCRβ Ab, within electronically gated B220 and CD8-negative lymphocytes. In other experiments, Ags were first equilibrium-loaded overnight onto B6.129-*Tcra*$^{o/o}$ splenocytes, and then mixed with C57BL/6 splenocytes magnetically depleted of MHC class II-positive cells. To directly evaluate iNKT cell division during culture, splenocytes were labeled with 2 μM CFSE (Molecular Probes) in PBS for 8 min at room temperature, followed by quenching with cold FCS and washing with ice-cold RPMI 1640 supplemented with 10% FCS before culture. Evaluation of iNKT cell proliferation was performed by multiplying the percentage of iNKT cells determined by flow cytometry with the total cell number.

Cell-free Ag dissociation assay

Soluble mouse CD1d1 was Ni-affinity purified, as described (44), and bound to ELISA plates at a concentration of 10 μg/ml. Following binding at 4°C for 18 h and blocking of unbound sites with 2% FCS, plate-bound soluble mouse CD1d1 was loaded with 0.1 μM lipids for 12 h at 37°C. After removing excess lipids, the Ag was allowed to dissociate for the indicated times at 37°C. The wells were washed again, and ~5 × 10⁴ hybridoma cells were added to each well. Controls included wells bound with 2 μg/ml anti-CD3ε (positive) or with 5 μg/ml BSA (negative) loaded with 1 μg/ml αGalCer. IL-2 secreted upon activation was monitored by ELISA. Data are presented as the percentage of maximum activation.

Determination of Hill coefficient

Hill coefficient was determined from epitope titration experiments. Briefly, CD1d1 and H2K^b-H28 tetramers or dimers were loaded with increasing amounts of glycolipid ligand or peptide epitopes, respectively. Note that H2K^b tetramers were initially folded with H28-derived epitope, a peptide with low affinity for H2K^b, allowing rapid and efficient ligand exchange (Y. Yoshimura and S. Joyce, unpublished data). Glycolipid and peptide loading occurred at 37°C and room temperature, respectively, for 16–18 h.

Hill curve was derived from data transformation: fractional saturation (Ys) of the receptor was determined as the ratio of specific MFI to maximum MFI (V_{max}) at a defined ligand concentration and plotted against the concentration of added ligand (glycolipid or peptide). Linear graph of logarithmic roots of the values for the x- and y-axes were used to determine the slope of the Hill curve revealing the Hill coefficient (34).

Results

The CD1d1-αGalCer/Va14Ja18 TCR interaction has high relative avidity

There are a number of different methods available to assess the kinetics and extent of ligand-receptor interactions. Biophysical methods using purified recombinant molecules have been extremely useful in the study of a variety of immunological receptors (45–47). That notwithstanding, methods that examine molecules on living cells are particularly powerful (24, 26, 28, 48, 49). To gain insight into the parameters that govern the binding interactions of the CD1d1 ligand to the specialized TCR of iNKT cells required for their activation, we first determined the K_{av} (measured affinity of tetrameric Ags for the cognate TCR) between tetrameric CD1d1-glycolipid Ag and its receptor on live cells. For comparison, the K_{av} of peptide Ags for the TCR expressed by recently activated CD8$^+$ T lymphocyte (CTL) clones specific for two H2K^b-restricted mH (H60 and H28 (27)) Ags and a viral (SV-40 T Ag-derived epitope IV (39)) Ag was measured. The comparison with class I-restricted Ags was used, because iNKT cells reflect memory/activated T lymphocyte phenotype similar to CTL clones.

CD1d1-αGalCer tetramer binds Va14Ja18$^+$ but not Va14-negative NKT hybridomas (Fig. 1A). Similarly, H2K^b-peptide tetramers specifically bind their cognate, but not irrelevant, CTL clones (data not shown and Refs. 38 and 39). Nonspecific binding was <5% in all cases (Fig. 1A and data not shown). From the binding isotherms, the K_{av} of Ag-TCR interaction was calculated (see *Materials and Methods*).

Va14Ja18 TCR binds CD1d1-αGalCer with a K_{av} ranging from 7 to 17 nM (Fig. 1B and Table I). TCR of conventional T cells bind H2K^b-peptide tetramers with a wide range of K_{av}, ranging from ~20 to 220 nM (Fig. 1C and Table I). Note that, in this study, the

saturation binding isotherms at equilibrium were derived at 4°C. Whereas the K_{av} values obtained at 4°C may not be the same as those at 37°C, the relationship of the K_{av} between different Ag-TCR interactions remains unaltered (50). Consistent with that reported (50), we also found that the K_{av} determined for two iNKT hybridomas at 4°C (N37-1H5a, 10.5 nM; N38-2C12, 18.8 nM) maintained their avidity relationship at 37°C (N37-1H5a, 39.3 nM; N38-2C12, 65.2 nM).

To obtain a more physiological estimate of the K_{av} between CD1d1-αGalCer and Va14Ja18 TCR, the above binding analysis was extended to NKT cell-enriched thymocytes and splenocytes. The K_{av} of CD1d1-αGalCer for Va14Ja18 TCR of live NKT cells (Fig. 1D and Table I) is similar to that observed with iNKT hybridomas (B and Table I). Taken together, the K_{av} of the CD1d1-αGalCer-Va14Ja18 TCR engagement is similar to or higher than that of immunodominant peptide Ag-TCR interaction.

Glycolipid Ag-Va14Ja18 TCR interaction is long-lived

Functional T cell responses following Ag recognition have been correlated with the dwell time, measured as the $t_{1/2}$ of ligand engagement by its receptor (28, 49, 51, 52). We found that the $t_{1/2}$ of glycolipid Ag/Va14Ja18 TCR is long, lasting between 10 and 40 min (Fig. 1E, top two panels; Table I), which is longer than the $t_{1/2}$ observed for peptide Ag/TCR interactions investigated (Fig. 1E, bottom panel; Table I). Hence, the off-rate of CD1d1-αGalCer/TCR interaction on the surface of intact NKT cells appears quantitatively distinct from that of conventional T lymphocytes.

Our data are consistent with previously published reports (28, 53) for studies of peptide-Ag-specific T cells. Due to the manner in which our experiments were performed and analyzed, the data may appear inconsistent with recent dwell-time measurements between CD1d1-αGalCer and iNKT cell receptors (26). Specifically, we did not use anti-CD1d1 or anti-MHC Abs in our experiments, and CD1d1-lipid or MHC-peptide levels detected postchase were not normalized to prechase reacted anti-TCRβ levels. Abs to MHC molecules added during the chase period prevent the dissociating monomers from reassociating with their receptor (49). In our experiments, $t_{1/2}$ of H60 tetramer for cognate TCR determined in the absence (9 ± 0.01 min; see Table I) or presence of an H2K^b-reactive Ab, EH144 (2–10 min; n = 5), was similar. Likewise, $t_{1/2}$ of CD1d1-αGalCer tetramers for cognate iNKT cell receptor determined in the absence (9.8 ± 0.9 min; n = 5) or presence of 100 μg/ml CD1d1-reactive Ab 1B1 (17.6 ± 7.4 min; n = 2) was similar. It should also be noted that, unlike MHC class II, which is not expressed by mouse T cells, MHC class I and CD1d1 are expressed by T lymphocytes. The use of anti-class I or anti-CD1d1 has the potential to cross-link the dissociating tetramer to the T cells, thereby skewing the data toward increased dwell time. Hence, the comparative off-rate measurements were performed in the absence of Abs.

We also found that the TCR levels on iNKT cells and CTL at time zero and at 120 min of chase were similar when they were stained with anti-TCRβ Ab postchase (data not shown). In contrast, prestaining with anti-TCRβ resulted in a significant loss of TCRβ staining during chase, most likely due to the $t_{1/2}$ of anti-TCRβ Ab and cell surface TCR interaction. Thus, we chose not to normalize the remaining CD1d1-αGalCer tetramer bound postchase to prechase reacted anti-TCRβ staining, as described in published reports (28, 53). Nevertheless, our results are consistent with the conclusion that iNKT cell receptor interaction with CD1d1-presenting glycolipid Ag exhibits longer dwell time than that of CTL receptor interaction with peptidic Ags (26).

FIGURE 1. Biochemical features of glycolipid Ag/ Val4Jal8 TCR and peptide Ag/TCR interactions. *A*, Ag-free and αGalCer-loaded CD1d1 tetramer were reacted with Val4-negative or iNKT hybridomas to determine the specificity of the reagent. *B–D*, Saturation binding isotherms were generated by reacting the indicated concentrations of CD1d1-αGalCer tetramers with four iNKT hybridomas (N37-1H5a, Vb8.2Jb2.6; N38-2C12, Vb8.2Jb2.5; N38-3C3, Vb8.2Jb2.2; and DN32.D3, Vb8.2Jb2.4) (*B*) or NKT cell-enriched thymocytes and splenocytes (*D*). Similar isotherms were generated using the indicated concentrations of H2K^b-peptide tetramers in a reaction with specific CTL clones (SV40 epitope IV-specific 2168T as well as mH Ag-specific SPH60, BH60 and SPH28) (*C*). All binding reactions were performed at 4°C in the presence of sodium azide to prevent ligand-induced capping and TCR internalization. Specific MFI in *B–D* measured by flow cytometry are represented as a fraction of maximum binding. K_{av} was calculated using the Michaelis-Menten equation (see *Materials and Methods*). *E*, To determine the $t_{1/2}$ of Ag-receptor binding, the indicated T cells were reacted with specific tetrameric Ag. After extensive washes, the dissociation of Ag from cells during the chase was monitored by flow cytometry. Specific MFI is represented as a fraction of that detected at the beginning of chase.
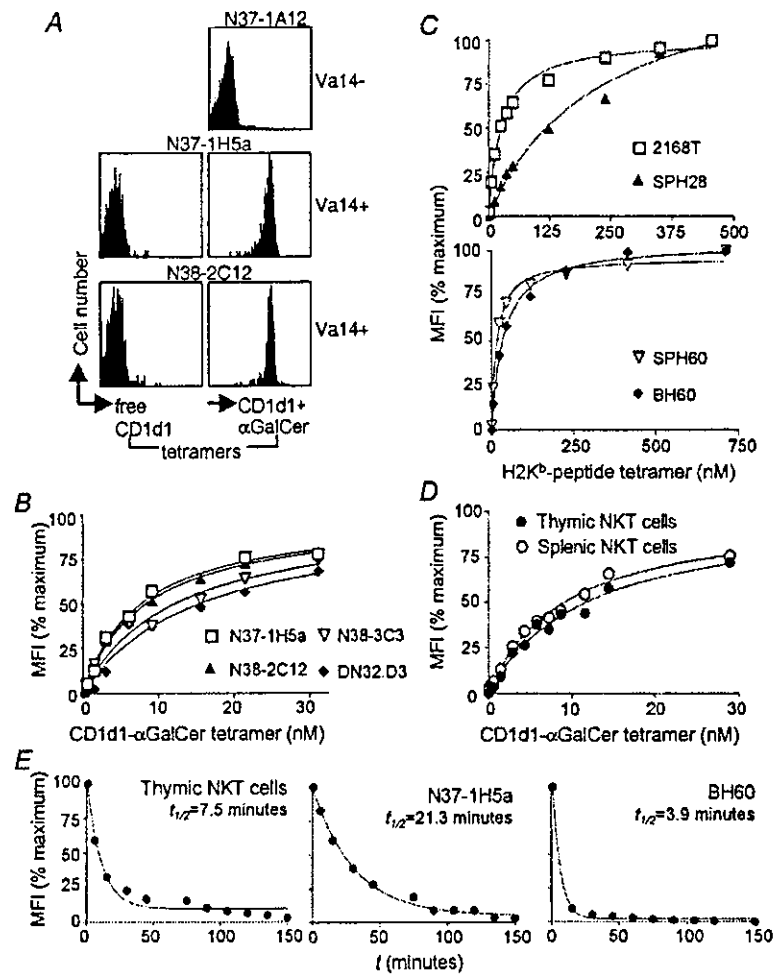
TCR β-chain repertoire of iNKT cells impacts Ag specificity and the K_{av} of their interaction

Altered glycolipid ligands derived from αGalCer elicit distinct functional responses from iNKT cells in vivo and in vitro (19). Recently, the TCR β-chain repertoire of iNKT cells was implicated in high-affinity dimeric CD1d1-αGalCer binding; the

Vb8.2^{+} iNKT cells have higher affinity for Ag than those that express Vb7 (27). Differences in TCR β-chain repertoire and/or the affinity for altered glycolipid ligands could explain the differential Ag specificity and functional outcomes. Tetramers of CD1d1-αGalCer and its analogues OCH, 3,4D, and NH were generated concurrently under saturating conditions. Tetramers of

Table I. *Kinetic parameters of Ag-TCR interactions*

T Cell	Reactivity[a]	K_d (nM)[b] ± SEM (n)[c]	$t_{1/2}$ (min at 37°C)[b] ± SEM (n)	Hill Coefficient (h)[b] ± SEM (n)	
				Tetramer	Dimer
iNKT hybridomas/CD1d1-αGalCer					
N37-1H5a	CD1d1 + self lipid	7.5 ± 0.3 (3)	19.1 ± 1.3 (5)	2.8 ± 0.4 (3)	
N38-2C12	CD1d1 + self lipid	8.5 ± 2.0 (4)	42.1 ± 4.3 (5)	2.8 ± 0.3 (3)	1.8 ± 0.2 (2)
DN32.D3	CD1d1 + self lipid	16.8 ± 0.9 (3)	37.3 ± 2.6 (2)	2.6 (1)	
N38-3C3	CD1d1 + self lipid	17.6 ± 3.4 (3)	16.4 ± 1.0 (2)	2.4 (1)	
C57BL/6 iNKT cells/CD1d1-αGalCer					
Thymic	CD1d1 + self lipid	10.7 ± 3.0 (4)	9.8 ± 0.9 (5)	2.5 ± 0.2 (3)	
Splenic	CD1d1 + self lipid	8.8 ± 0.7 (4)	11.4 ± 0.6 (3)	2.7 ± 0.2 (3)	
Conventional CD8^{+} T lymphocytes/H2K^b-peptide					
2168T	H2K^b + epiIV	23.9 ± 2.7 (3)	ND	1.1 ± 0.1 (4)	
SPH60	H2K^b + H60	20.4 ± 2.9 (3)	9.4 ± 0.03 (2)	1.0 ± 0.1 (3)	1.0 ± 0.2 (2)
BH60	H2K^b + H60	33.4 ± 1.7 (3)	3.9 ± 0.01 (2)	0.9 ± 0.04 (3)	
SPH28	H2K^b + H28	216.7 ± 9.2 (4)	2.1 ± 0.9 (2)	ND	

[a] The reactivities of all of the T lymphocytes have been described (see *Results* for references).
[b] Calculations of the kinetic parameters are described in *Materials and Methods* (also see *Results* for details).
[c] *n*, Number of experimental values.

FIGURE 2. CD1d1-OCH is recognized with lower K_{av} but similar dwell time compared with CD1d1-αGalCer by a Vb8.1,8.2-skewed iNKT cell repertoire. *A,* Equimolar quantities (30 nM) of CD1d1-glycolipid tetramers were reacted with a Val4-negative (N37-1A12) or two iNKT (N37-1H5a and N38-3C3) hybridomas, and NKT cell-enriched thymocytes. *B,* Expression of TCRβ, Vb8.1,8.2, or Vb7 on CD1d1-αGalCer and -OCH tetramer-positive, electronically gated HSA^low CD8^low thymocytes. *C,* Expression of TCRβ, Vb8.1,8.2, or Vb7 on CD1d1-αGalCer and -OCH tetramer-positive, magnetically sorted NK1.1⁺ thymocytes. *D* and *E,* Saturation binding isotherms were generated using iNKT hybridomas and NKT cell-enriched thymocytes and splenocytes reacted with the indicated concentrations of CD1d1-αGalCer or -OCH tetramers. Similar binding isotherms were generated using Vb8.1,8.2⁺ and Vb7⁺ splenic iNKT cells. From the binding isotherms, K_{av} was calculated as described in Fig. 1. *F,* $t_{1/2}$ of CD1d1-αGalCer and CD1d1-OCH binding to thymic iNKT cells was determined as described in Fig. 1. Binding reactions in A–E were performed at 4°C in the presence of sodium azide to prevent capping and internalization.
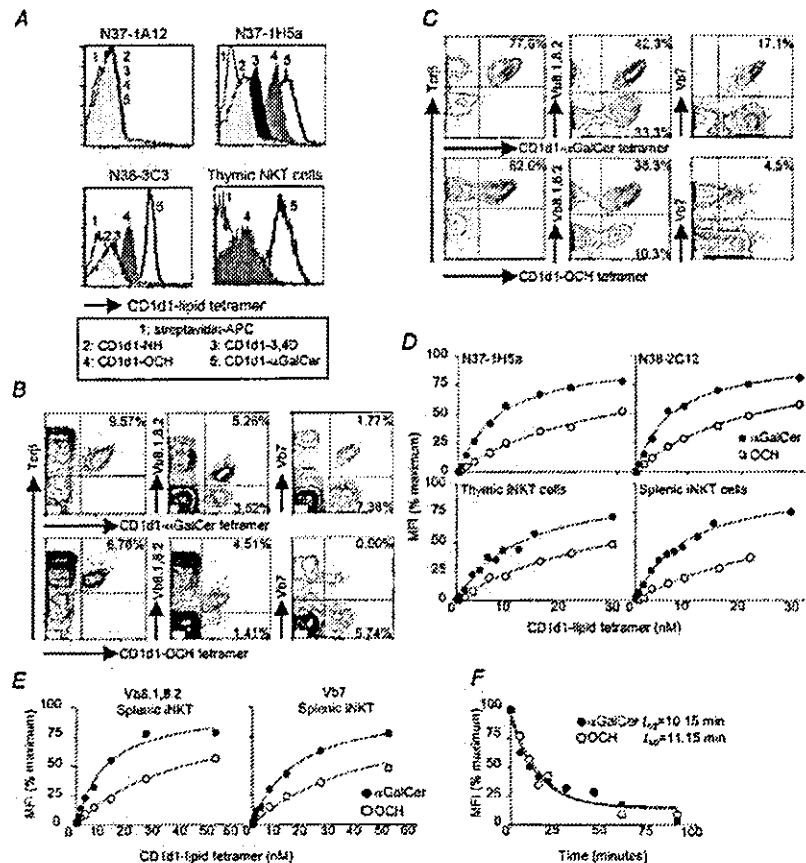
CD1d1-αGalCer, -OCH, and -3,4D have exquisite specificity for iNKT cells (Fig. 2A). However, CD1d1-3,4D (an analogue lacking the two hydroxyl groups at C atoms 3 and 4 of the long-chain base) and especially CD1d1-NH (C atom 2′ amine-modified αGalCer) bind poorly or not at all, respectively, to iNKT hybridomas (Fig. 2A).

To determine the TCR β-chain repertoire of iNKT cells recognizing OCH, bulk (Fig. 2B) and sorted NK1.1⁺ (C) thymocytes were reacted with CD1d1-αGalCer or CD1d1-OCH tetramers and TCRβ-, Vb8.1.8.2-, or Vb7-specific Abs. Surprisingly, CD1d1-OCH tetramer detected ~30% fewer total iNKT cells compared with CD1d1-αGalCer tetramer (Fig. 2, B and C). Interestingly, a large majority of CD1d1-OCH tetramer-positive cells expressed Vb8.1,8.2; they reflected 85–90% of CD1d1-αGalCer tetramer-reactive cells (Fig. 2, B and C). Furthermore, Vb8.1,8.2-negative and Vb7⁺ iNKT cells inefficiently reacted with CD1d1-OCH tetramer (25–50% of CD1d1-αGalCer tetramer-positive cells). However, TCR β-chain usage for CD1d1-3,4D-reactive cells could not be determined, because the MFI of this interaction was very low, and hence, it was difficult to resolve positive from negative staining. These results for the first time directly demonstrate that TCR β-chain repertoire of iNKT cells in vivo impacts their Ag binding. This difference could be a result of differing avidities of the altered

Table II. *Kinetic parameters of glycolipid Ag analogue/TCR interactions*

T Cell	K_d (nM) ± SEM (n)[a]			$t_{1/2}$ (min at 37°C)[b] ± SEM (n)		Hill Coefficient (h) ± SEM (n)	
	αGalCer[c]	OCH	3,4D	αGalCer[c]	OCH	αGalCer[c]	OCH
iNKT hybridomas							
N37-1H5a	7.5 ± 0.3 (3)	29.9 ± 0.3 (2)	ND	10.7 ± 3.0 (4)	ND	2.8 ± 0.4 (3)	2.2 ± 0.4 (2)
N38-2C12	8.5 ± 2.0 (4)	22.1 ± 1.7 (2)	ND	42.1 ± 4.3 (5)	ND	2.8 ± 0.3 (3)	2.3 ± 0.4 (2)
C57BL/6 iNKT cells							
Thymic							
TCRβ⁺	10.7 ± 3.0 (4)	31.2 ± 0.4 (2)	59.5 ± 3.1 (2)	9.8 ± 0.9 (5)	13.0 ± 1.9 (2)	2.5 ± 0.2 (3)	ND
Vb8.1,8.2⁺	10.5 ± 0.1 (2)	35.7 ± 1.9 (2)					
Vb7⁺	16.0 ± 0.8 (2)	46.6 ± 1.8 (2)					
Splenic	8.8 ± 0.7 (4)	27.4 ± 10.9 (2)	ND	ND	ND	2.7 ± 0.2 (3)	ND
Splenic C57BL/6 iNKT cells expanded with glycolipid Ag stimulation (96 h)							
αGalCer	9.1 ± 0.4 (2)	44.2 ± 2.9 (2)					
OCH	9.1 ± 0.6 (2)	39.7 ± 7.2 (2)					
3,4D	6.4 ± 0.5 (2)	25.1 ± 1.9 (2)					

[a] n, Number of experimental values.
[b] Calculations of the kinetic parameters are described in *Materials and Methods* (also see *Results* for details).
[c] αGalCer data is the same as presented in Table 1.

lipids for their TCR. Therefore, CD1d1-αGalCer, -OCH, and -3,4D tetramers were used to determine their K_{av} for the TCR. CD1d1-OCH binds iNKT TCR with about 3- to 4-fold lower K_{av} compared with CD1d1-αGalCer, whereas CD1d1-3,4D had a 6-fold lower K_{av} (Fig. 2D and/or Table II).

Considering that the TCR β-chain repertoire of cells recognizing OCH was Vb8.1,8.2 skewed, we hypothesized that TCR β-chain of the iNKT cell receptor impacts K_{av} for Ag. We found that Vb7⁻ iNKT cells have 50% lower K_{av} for both CD1d1-αGalCer and -OCH compared with Vb8.1,8.2⁺ iNKT cells (Fig. 2E and Table II). Note that K_{av} determination was performed with Vb7⁺ cells that detectably bound CD1d1-OCH tetramer, which represented only ∼50% of total CD1d1-αGalCer tetramer-reactive Vb7⁻ iNKT cells. Therefore, the results potentially represent a higher K_{av} than that of the entire Vb7⁺ iNKT population. Because the dwell time of TCR and Ag interaction correlates with the capacity for T cell activation, the $t_{1/2}$ of CD1d1-αGalCer, and CD1d1-OCH from iNKT cell receptor was determined as described above. The results indicate that both glycolipid Ags have similar dwell times for their cognate receptors (Fig. 2F and Table II). Taken together, the data suggest that the TCR β-chain repertoire and the K_{av} of Ag-receptor interaction, but not the dwell time, might govern distinct functional outcomes from iNKT cells.

iNKT cells recognize OCH and αGalCer in vivo with similar sensitivity

A number of in vitro studies have indicated that iNKT cells recognize CD1d1-αGalCer with nanomolar sensitivity (10–12, 14, 35). Ags with different binding affinity for their TCR activate T cells with distinct activation thresholds (54–58). To determine the sensitivity of effector responses by iNKT cells in vivo, C57BL/6 mice were injected i.v. with αGalCer and OCH, and serum cytokine response was measured after 90 min. CD1d1-restricted NKT cell (B6.129-*CD1d1*$^{O/O}$)- and iNKT cell (B6-*Ja18*$^{O/O}$)-deficient mice do not respond to these glycolipids (Fig. 3A), nor do C57BL/6 mice injected with the vehicle used to dissolve the glycolipid Ags (data not shown).

Mice administered 0.5 μg of OCH elicited substantial amounts of IL-2 and IL-4; TNF-α, IL-13, and CSF-2 (GM-CSF) were also detectable within 90 min (Fig. 3A). Administration of 1.0 μg of αGalCer or OCH elicited a robust cytokine response including TNF-α, IL-13, and CSF-2 (Fig. 3A). Note that the observed IFN-γ response is at the very low end of maximum at this early time point. Furthermore, the previously reported differential IFN-γ response to OCH and αGalCer are strikingly apparent only at or after 6 h (19), because that is the time point at which IFN-γ peaks (59). Thus, at early time, αGalCer and OCH are recognized with similar sensitivity in vivo.

Kinetics of CD1d1 loading with αGalCer and OCH explain similar early iNKT cell response in vivo

Activation of T cells is an effect of Ag-TCR engagement and consequent intracellular signaling. T cell activation correlates with the extent of receptor down-regulation due to signal-dependent altered intracellular TCR trafficking (60–62). Surprisingly, iNKT cells respond to αGalCer and OCH with similar early sensitivity (Fig. 3A), despite different equilibrium binding properties of TCR and specific Ag (Fig. 2, D–F, and Table II). To determine the cellular basis of αGalCer and OCH sensitivity, the kinetics and extent of TCR down-regulation following addition of increasing concentrations of αGalCer and OCH to splenocytes in vitro were evaluated. Both αGalCer and OCH down-regulated similar levels of surface TCR within 4–12 h of Ag stimulation (Fig. 3B, top three panels). However, αGalCer was ∼10-fold more potent at inducing surface

TCR down-regulation after 24 h of stimulation. Thus, the kinetics of TCR down-regulation reflected the early induced iNKT cell response in vivo.

Two plausible mechanisms can explain the difference observed in early and late iNKT cell responses to αGalCer and OCH. αGalCer, because of its higher K_{av} for Val4Ja18 TCR compared with OCH, is a more potent iNKT cell ligand resulting in more sustained TCR down-regulation and activation. Alternatively, OCH, because of its shortened sphingosine and acyl chains, binds CD1d1 faster than αGalCer, and hence compensates for its low K_{av} and elicits an early iNKT cell response. To distinguish between the two possibilities, B6.129-*Tcra*$^{O/O}$ splenocytes, which lack T and iNKT cells, were incubated with increasing quantities of αGalCer and OCH for 24 h. They were then used to stimulate C57BL/6 splenocytes depleted of MHC class II-positive cells, after which iNKT cell receptor down-regulation was evaluated. OCH was 10- to 20-fold less efficient in TCR down-regulation compared with αGalCer at all time points tested (Fig. 3C). This result is consistent with the hypothesis that αGalCer and OCH have different kinetics of CD1d1 loading, and that the similar early iNKT cell response to the two Ags in vivo reflects rapid on-rate of OCH compared with αGalCer.

To determine the concentration threshold required for the elicitation of distinct cytokines from iNKT cells by αGalCer and its analogue OCH, C57BL/6 splenocytes were stimulated with increasing concentrations of these glycolipids. The results revealed that IL-2 and IFN-γ response after 48 h (Fig. 3D) required at least 50% iNKT cell receptor down-regulation measured at 24 h (B, bottom panel) and medium Ag concentration threshold of αGalCer and OCH (D). In contrast, secretion of CSF-2 and IL-4 was more sensitive to low concentrations of glycolipid Ags and, hence, responded to low levels of TCR down-modulation (Fig. 3, B and D). In support of our previous report (19), OCH preferentially induced an IL-4 response, whereas 50-fold higher concentration of OCH was required to produce an IFN-γ response similar to that induced by αGalCer (Fig. 3D). Thus, the secretion of cytokines by iNKT cells follows a hierarchical Ag response pattern, with higher avidity and higher concentrations required for secretion of IFN-γ and IL-2 compared with both low avidity and low concentration for CSF-2 and IL-4.

To fully understand the properties of CD1d1-OCH interaction, we used a cell-free Ag presentation assay to determine its dissociation kinetics. Plate-bound soluble CD1d1 was loaded with equimolar quantities of αGalCer or OCH. After removing unbound lipid, the complexes were allowed to dissociate for varying time periods at 37°C. The $t_{1/2}$ of Ag-CD1d1 complex was monitored by its ability to activate iNKT cell hybridomas. OCH interaction with CD1d1 was more labile, because it dissociated faster than αGalCer from CD1 (Fig. 3E). Thus, similar early sensitivity of iNKT cells to αGalCer and OCH in vivo reflects the differences in the kinetics of their interaction with CD1d1 and also the differences in their equilibrium parameters of TCR engagement.

Activation of iNKT cells by 3,4D in vitro causes selective expansion of high-avidity clones

The altered lipid ligand, 3,4D, engages the iNKT cell receptor, albeit with low K_{av} compared with αGalCer and OCH (Fig. 2B and Table II), and elicits a weak cytokine response in vivo (19). To elucidate the biochemical basis of this weak response, the proliferative capacity of iNKT cells to Ag engagement was determined in vitro by CFSE dye dilution assay. After stimulation of splenocytes with Ags for 96 h, iNKT cells were costained with CD1d1-αGalCer tetramer and TCRβ-specific Ab. At high concentration (575 nM), αGalCer, OCH, and 3,4D induced extensive iNKT cell

FIGURE 3. Kinetics of CD1d1 loading with αGalCer and OCH explain similar early iNKT cell response in vivo to the two glycolipids. A, C57BL/6 mice or control B6.129-$CD1d1^{0/0}$ and B6-$Ja18^{0/0}$ mice were injected i.v. with the indicated concentrations of αGalCer, OCH, or vehicle. After 90 min, serum cytokines were monitored. Background cytokine level (<3%) elicited by vehicle-treated mice was subtracted from the Ag-treated response. The data represent cytokine responses (±SE) elicited by four individual mice in two identical experiments. B, Va14Ja18 TCR down-regulation was monitored at the indicated time points following addition of αGalCer or OCH to C57BL/6 splenocytes. iNKT cell receptor level was determined by flow-cytometric analysis following reaction with CD1d1-αGalCer tetramer and anti-TCRβ Ab, within electronically gated B220 and CD8-negative lymphocytes. C, Va14Ja18 TCR down-regulation was monitored following reaction of C57BL/6 splenocytes magnetically depleted of MHC class II-positive cells with B6.129-$Tcra^{0/0}$ splenocytes equilibrium loaded with Ag overnight. D, Cytokines elicited by C57BL/6 splenocytes were monitored 48 h following addition of indicated quantities of αGalCer or OCH in vitro by sandwich ELISA. E, The dissociation of αGalCer and OCH from plate-bound soluble CD1d1 was monitored after removing excess glycolipids, and chasing the Ag for 4, 12, 24, and 36 h at 37°C, using an iNKT cell hybridoma, N38-2C12, as a probe. Activation-induced IL-2 was determined and plotted as percentage of maximum, a value obtained at start of chase.
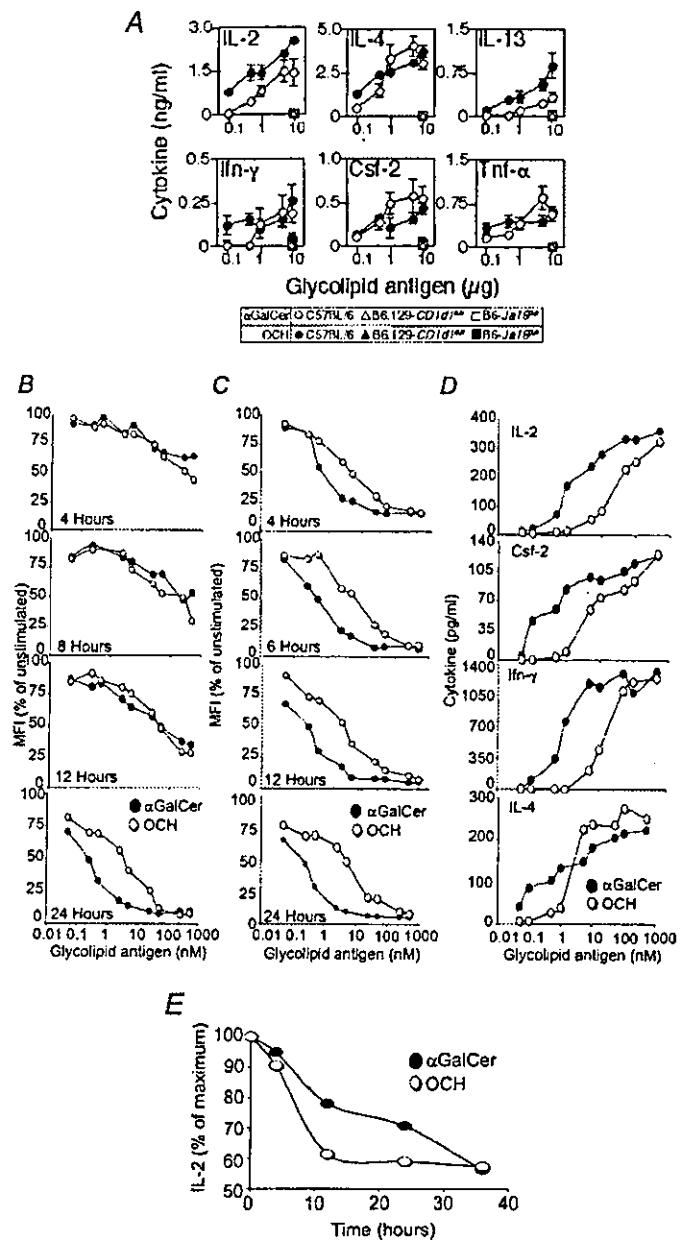
proliferation (Fig. 4A). In contrast, at a lower concentration (2.9 nM) of these same Ags, αGalCer induced a strong proliferative response; OCH induced a partial proliferative response, whereas 3,4D and NH elicited a very weak or no response, respectively (Fig. 4A). Furthermore, quantitation of the proliferative response revealed that αGalCer induced maximum proliferation at 5.75 nM, and OCH at 57.5 nM, whereas maximum expansion was not reached even with 575 nM of 3,4D (Fig. 4B). We also noted that stimulation with supraoptimal Ag concentrations does not result in increased proliferation, but actually reduces total iNKT cell expansion (Fig. 4B).

Together, the data reveal that, despite differences in K_{av} and the TCR β-chain repertoire, the altered lipid ligands induce proliferative response (Figs. 2, B-F, and 4, A and B). Therefore, the β-chain repertoire and the K_{av} of Ag-expanded iNKT cells were determined. TCR β-chain repertoire of iNKT cells following αGalCer, OCH, and 3,4D stimulation remains largely unaltered at

Ag concentrations inducing a maximum proliferative response, although a slight decrease in the percentage of Vb8-negative iNKT cells was noted (~35% of expanded iNKT (Fig. 4C) compared with ~45% for naive iNKT cells (Fig. 2B)). Additionally, very little if any difference was observed in the Vb repertoire of iNKT cells expanded with different suboptimal doses of αGalCer and OCH (data not shown). Interestingly, iNKT cell activation by 3,4D, but not αGalCer or OCH, resulted in the expansion of iNKT cells responding to Ag with higher K_{av} for αGalCer and OCH (Fig. 4D and Table II). Thus, high-avidity iNKT cells preferentially expand to suboptimal TCR engagement.

Cooperative glycolipid Ag recognition by iNKT cells

Self-Ag recognition must be finely tuned to prevent iNKT cell activation during physiological conditions, but respond rapidly to disturbances in cellular physiology. In other words, iNKT cells need to be very sensitive to modest changes in Ag concentration.

FIGURE 4. Activation of iNKT cells by suboptimal avidity Ag 3,4D in vitro causes selective expansion of high-avidity clones. *A*, C57BL/6 splenocytes were stimulated with the indicated concentrations of glycolipid Ags for 96 h. iNKT cell number and cell division history were determined using tetramers and CFSE (see *Materials and Methods*). *B*, Total iNKT cell number was determined following 96 h of Ag-stimulated culture. *C*, TCR β-chain repertoire of CD1d1-αGalCer- and -OCH-reactive cells following 96 h of in vitro iNKT cell stimulation with indicated concentrations of glycolipid Ags. *D*, C57BL/6 splenocytes were stimulated with the indicated glycolipid. The resulting iNKT cell population was reacted with the indicated concentration of CD1d1-αGalCer or CD1d1-OCH tetramers. From the binding isotherms, K_{av} was determined as described in Fig. 1. Binding reactions were performed at 4°C in the presence of sodium azide to prevent capping and internalization.
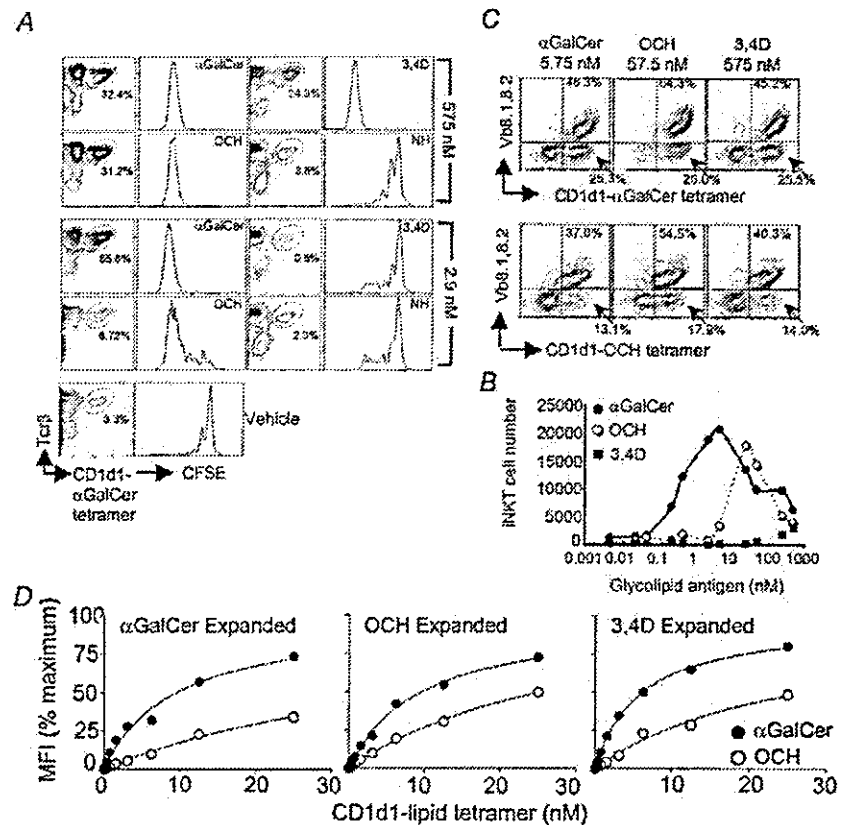
In biological systems, this kind of fine-tuning is often achieved by using cooperative ligand-receptor interactions (33, 63). To determine whether cooperativity participates in sensitive glycolipid Ag recognition, this mode of interaction was determined by calculating the Hill coefficient (see *Materials and Methods*). The Hill coefficient of the interaction between the tetrameric Ag and the iNKT cell receptor was >2 (Fig. 5*A* and Table I). In stark contrast, all MHC class I-restricted TCR had a calculated Hill coefficient of ~1 (Fig. 5*B* and Table I), indicating a lack of cooperativity. Peptide binding to each H2K^b monomer of the tetrameric molecule is an independent event. Saturation binding of the tetramer to the TCR with increasing concentration of added peptide indicates occupancy of all four sites (Fig. 5*B*). Furthermore, an analysis of the stoichiometry of class I H chain, β_2-microglobulin, and peptide following ligand exchange by Edman sequence determination (64) revealed a 1:1:1 ratio of the three components (data not shown). Thus, a Hill coefficient of 1 is not due to incomplete loading of the class I tetramer.

OCH is a structurally different Ag, particularly in the hydrophobic component thought to interact with CD1d1. Also, OCH interaction with CD1d1 has distinct kinetic parameters compared with αGalCer (Figs. 2*F* and 3*E*). Thus, to exclude the possibility that the biochemical or structural properties of αGalCer loading onto CD1d1 account for the observed cooperative response, Hill coefficient was measured for the binding of CD1d1-OCH to the Va14Ja18 TCR. As expected, we found that the Hill coefficient for CD1d1-OCH and CD1d1-αGalCer for the same Va14Ja18 TCR are very similar (Fig. 5*C* and Table II). Thus, Hill coefficient measurement does not reflect the loading properties of glycolipid Ags, but rather, it is the property of the Ag receptors with which it interacts.

To independently demonstrate cooperative Ag engagement by iNKT cells with multimeric Ags other than soluble, biotinylated monomers of CD1d1 and H2K^b prepared in-house, we determined the Hill coefficients with commercially obtained dimeric IgG1-CD1d1 and IgG1-H2K^b fusion molecules loaded with αGalCer and H60 peptide, respectively, for iNKT cells and H60-specific SPH60 CTL clone. iNKT cells demonstrated cooperative engagement of both dimeric and tetrameric Ag by the Va14Ja18 TCR (Fig. 5*D* and Table I). As expected, neither dimeric nor tetrameric H2K^b cooperatively engaged their cognate TCR (Fig. 5*D* and Table I). Thus, we conclude that, in contrast to conventional T lymphocytes, glycolipid Ag recognition by iNKT cells involves cooperativity.

iNKT cell receptor appears to have distinct structure and/or organization

A plausible model for cooperative tetrameric Ag engagement by Va14Ja18 TCR is receptor partitioning and oligomerization within lipid rafts (50). To test this model, Hill coefficients for Ag-receptor interactions were determined for two representative iNKT hybridomas (N38-2C12 and N37-1H5a). NKT cell-enriched thymocytes, and two CTL clones (SPH60 and BH60), following disruption of their lipid rafts. Lipid rafts were disrupted by cholesterol depletion with methyl-β-cyclodextrin (65) or alternatively by filipin-mediated intercalation of this membrane microdomain (66). Disruption of lipid rafts did not alter the Hill coefficient for any of the interactions tested (data not shown), suggesting that these membrane microdomains are not critical for cooperative Ag engagement by iNKT cell receptor.

To further examine the structural properties of iNKT cell Ag receptor, we used fluorescence resonance energy transfer (FRET)

FIGURE 5. Cooperative engagement of multimeric CD1d1 by the Val4Ja18 TCR. A constant concentration of multimer (CD1d1 tetramer (*A* and *C*); H2K^b tetramer (*B*); CD1d1 and H2K^b dimers and tetramers (*D*)) was loaded with the indicated concentrations of Ag (αGalCer or OCH (*A* and *C*); peptide (*B*)) and reacted with freshly isolated NKT cell-enriched thymocytes (*A*), NKT hybridomas (*A* and *C*), or CTL clones (*B*). Binding was monitored as described in Fig. 1. From the binding curve, Hill plots and Hill coefficients (*h*), represented beneath the Ag-binding curves, were derived (see *Materials and Methods*). Tetramers of CD1d1 and H2K^b were generated by fluorochrome-conjugated streptavidin-mediated tetramerization of biotinylated monomers. Binding of dimers of CD1d1 and H2K^b, owing to their fusion to IgG1 H chains, were detected with Alexa Flour 647- or PE-conjugated Fab specific for the Fc portion. The high regression coefficient (>0.90) for all Hill plots indicates that the calculated *h* values are significant. All binding reactions were performed at 4°C in the presence of sodium azide to prevent capping and internalization.
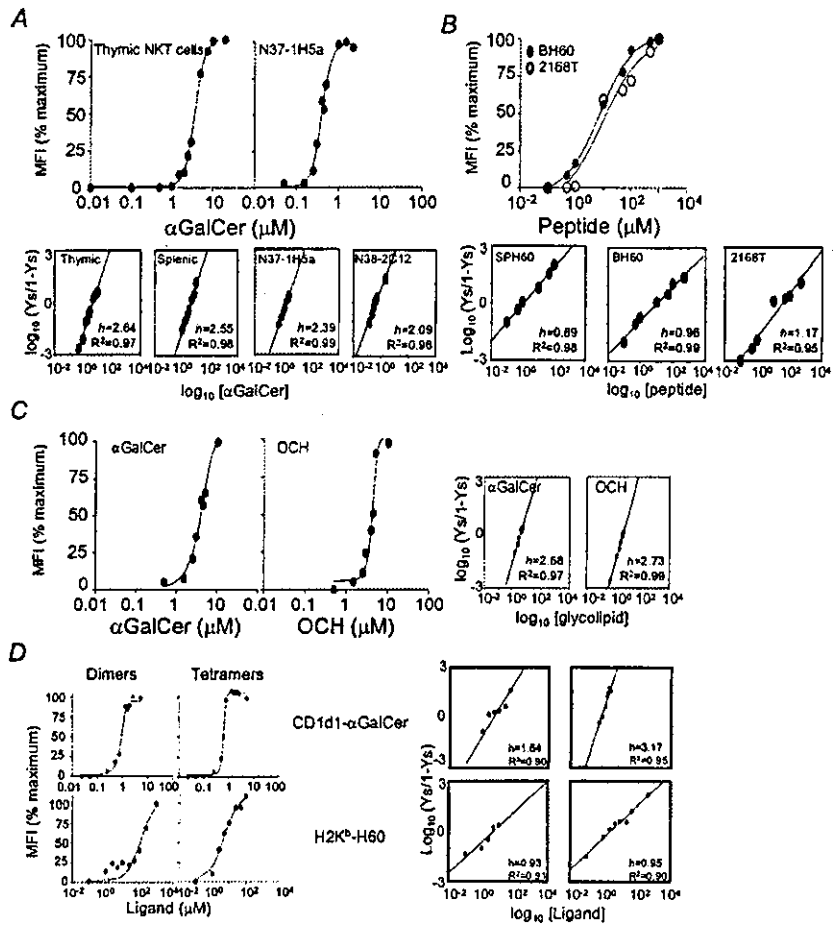
measurements between CD1d1 and H2K^b multimers and Abs specific for components of the TCR complex. In the course of our studies, we observed that costaining of iNKT cells ex vivo by allophycocyanin- or PE-conjugated CD1d1 tetramers and PE- or allophycocyanin-TCRβ (clone H57-597) or anti-CD3ε (clone 145-2C11) Abs resulted in large and repeatable increase in FL3 channel fluorescence in a properly compensated flow-cytometric experiment (Fig. 6, *A* (iNKT cell hybridoma N38-2C12) and *B* (thymic iNKT cells)). Such large FRET shift was not observed with high-intensity staining Abs specific for cell surface molecules not within the TCR complex (e.g., anti-CD44, clone IM7; Fig. 6). As PE and allophycocyanin have overlapping fluorescence emission and absorption spectra, respectively, it was likely that this result was a consequence of nonradiative FRET. This hypothesis was tested by running samples on the flow cytometer with the red diode laser (emission, 635 nm) and its FL4 filter switched off. Indeed, we still observed FL3 fluorescence only when costaining with CD1d1 multimers and TCR complex-specific Abs. The large FRET observed upon tetramer-anti-TCRβ/anti-CD3ε binding to iNKT cells presented an opportunity to test the hypothesis that the structural orientation and/or organization of Val4Ja18 TCR are distinct from αβ TCR of conventional CTL. When H60-specific CTL were costained in a manner identical with that of iNKT cells, and analysis was restricted to equivalent MFI of anti-TCRβ or anti-CD3ε and H2K^b multimer, very little FRET was detected (Fig. 6A). Similarly, we observed FRET using PE-conjugated CD1d1 tetramers and allophycocyanin-conjugated anti-TCRβ or anti-CD3ε Abs (data not shown). FRET between CD1d1-αGalCer tetramers and

TCRβ on iNKT cells directly correlated with the staining intensity, even at relatively low concentrations (~2.5 nM; Fig. 6C). In contrast, no FRET between H2K^b tetramers and TCRβ or CD3ε was observed, even with saturating concentrations of H2K^b tetramers (~250 nM; Fig. 6C). FRET is exquisitely sensitive to small changes in donor and acceptor fluorochrome distances (FRET, $\sim r^6$). Thus, these results strongly suggest that iNKT cell receptor has a distinct structure and/or organization, resulting in shorter distance between donor and acceptor fluorochromes used.

Discussion

In summary, our findings demonstrate that iNKT cell receptors recognize glycolipid Ags with avidities similar to, if not higher than, those of immunodominant, high-affinity αβ TCR of conventional T cells. In contrast to CTL, which recognize Ag over a large avidity range (20–220 nM), iNKT cells efficiently recognize Ag within a narrow window of avidity (10–40 nM). Interestingly, although the TCR-Ag dwell time for αGalCer and OCH are very similar, TCR down-regulation as well as the proliferative and cytokine response of iNKT cells to these Ags directly correlated with avidity for Ag. Strikingly, both αGalCer- and OCH-bound CD1d1 tetramers and dimers display cooperative engagement of the iNKT cell receptor, a property that CTL clones tested in this study lack. Additional data revealed FRET between specific combinations of fluorochromes conjugated to CD1d1 tetramers or dimers (data not shown) and TCR β-chain or CD3ε-specific Abs. These findings
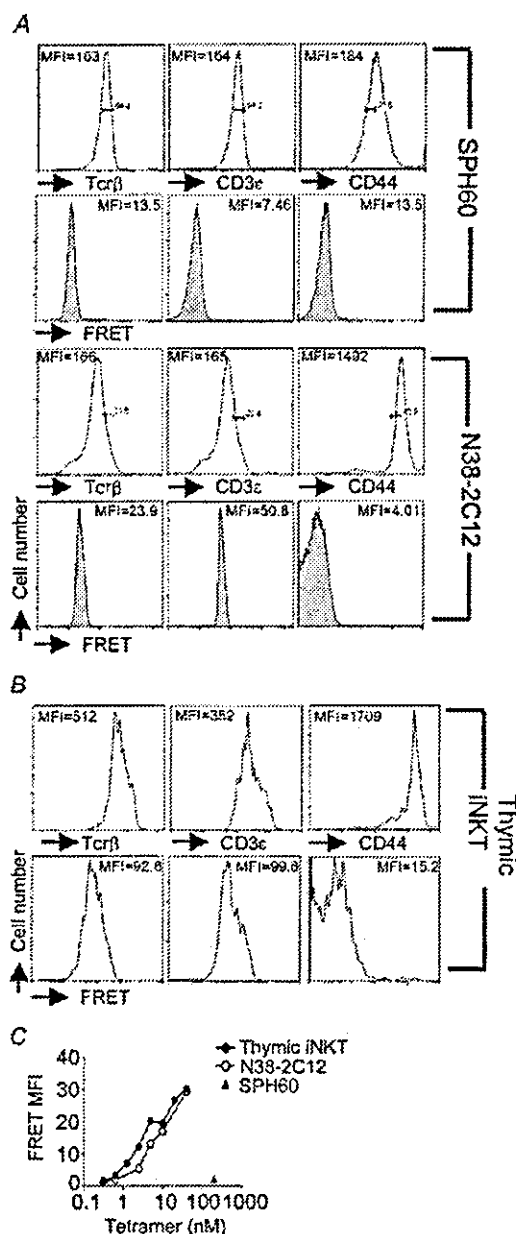
FIGURE 6. iNKT cell receptor has distinct structure and/or organization. CTL clone SPH60 (*A*), iNKT hybridoma N38-2C12 (*A*), and thymic iNKT cells (*B*) were reacted with allophycocyanin-conjugated H2K^b-H60 and CD1d1-αGalCer tetramers, respectively. They were also reacted with PE-conjugated Abs against TCRβ (H57-597; specific for TCRβ chain FG loop), CD3ε, or CD44. FRET was measured as the fluorescence in the FL3 channel, with the red diode laser off. CD1d1- and H2K^b-tetramer concentrations were adjusted to obtain equal MFI of tetramer staining. Considering that the 488-nm emission of the argon-ion laser cannot excite allophycocyanin, fluorescence detected in the FL3 channel is due to FRET-mediated allophycocyanin excitation. FRET-induced fluorescence intensity is indicated as a function of CD1d1-αGalCer tetramer concentration (*C*). All binding reactions were performed at 4°C in the presence of sodium azide to prevent capping and internalization.

suggest that the iNKT cell receptor structure and/or organization may be distinct from conventional αβ TCR.

Conventional T cells recognize peptide Ags with a wide range of avidities and dwell times (23–25, 28, 29). In contrast, strong

recognition of αGalCer and OCH, poor recognition of 3,4D, and no recognition of NH (19), by the Val4Ja18 TCR with distinct K_{av} points toward a narrow kinetic window for iNKT cell activation. We demonstrate that both optimal Ag concentration and relative avidity are essential to elicit a strong proliferative response by iNKT cells. Interestingly, as observed with conventional T cell effector functions (56), iNKT cells exhibit hierarchical functional consequences to Ag quality and concentration. In support of our previous study (19), we also find a dissociation from a clear avidity-concentration dependence in IL-4 secretion following OCH compared with αGalCer stimulation. Both low Ag concentration and low K_{av} are sufficient for selective IL-4 secretion and iNKT cell proliferation. In contrast, higher K_{av} and Ag concentration are required for IFN-γ response. Consistent with this conclusion is the finding that dendritic cells presenting a high concentration of the high K_{av} Ag αGalCer induce sustained IFN-γ response from iNKT cells (67). In this regard, iNKT cell response closely follows the principle of Ag concentration threshold set for IFN-γ and IL-4 responses elicited by conventional T cells (68).

Due to their potent immunoregulatory properties, therapeutic modulation of iNKT cell number and functional responses has been proposed for prevention of autoimmunity as well as for the enhancement of immune responses to tumors and vaccines. In the nonobese diabetic mouse model of autoimmune type I diabetes, iNKT number and function are low (43, 69, 70). Increasing the iNKT cell number (71–73) or the αGalCer treatment-induced Th2 bias (17, 18, 74) effectively reduces the incidence of type I diabetes in nonobese diabetic mice. Our data demonstrate that distinct glycolipid administration regimens may be required to induce tolerizing activity compared with IFN-γ-dependent antitumor and adjuvant properties of iNKT cells.

The natural self-Ag recognized by iNKT cells and its structural relationship to αGalCer remain unknown. However, we recently discovered that a cell line deficient in β-glucosylceramide (βGlcCer) is defective in the presentation of a self-Ag to iNKT cell hybridomas (15). Together with the evidence that the defect was not due to altered folding, intracellular traffic of CD1d1, or recognition of βGlcCer itself, these results suggest that βGlcCer is either a precursor or an essential factor in the synthesis and/or loading of a natural Ag. Thus, it is possible that the elusive self-Ag may be αGlcCer or a similar compound. Further support for the hypothesis that a self-Ag similar to αGalCer is recognized is the finding that transgenic overexpression of CD1d1 results in preferential deletion of Vb8.1,8.2$^+$ iNKT cells (75). This result is fully consistent with our finding that Vb8.1,8.2$^+$ iNKT cells have a higher K_{av} for αGalCer and OCH than Vb8.1,8.2-negative iNKT cells. Furthermore, the high K_{av} binding of CD1d1-αGalCer with Vb8.1,8.2$^+$ Val4Ja18 TCR is consistent with the high K_{av} binding of dimeric Ag to similar TCR (27). Importantly, for the first time, we demonstrate that the repertoire and Ag K_{av} of iNKT cell receptors are regulated during proliferation and result in selection of high-avidity iNKT cells under conditions of suboptimal stimulation. These data, taken together, suggest that the narrow kinetic window of recognition of αGalCer and its analogues is reflective of the parameters of natural self-Ag recognition.

The 2C transgenic TCR exhibits differing peptide Ag binding modes on naive and effector cells, suggesting cooperativity (50). The existence of two TCR αβ molecules within a single CD3 complex was evoked to explain this result (50). However, recent data suggest that the stoichiometry of TCR αβ assembly with CD3 complex is 1:1 (76). Whether this stoichiometry changes during CTL activation remains to be established. Using tetramers of CD1d1 and H2K^b, we demonstrate cooperative Ag engagement of glycolipid Ags by iNKT cell receptors but not that of peptidic Ags

by conventional $\alpha\beta$ TCR. The binding mode of 2C transgenic TCR was investigated using an IgG1-H2K^b dimer, and evidence for TCR $\alpha\beta$ dimerization was obtained by data deconvolution. To confirm the cooperative engagement of glycolipid Ag, we also used IgG1-CD1d1 and IgG1-H2K^b dimer similar to that used to investigate the 2C TCR (50). The results supported cooperative Ag engagement by iNKT cell, but not CTL receptors. Thus, the relationship of our findings with those previously reported is unclear.

Because H2K^b and CD1d1 tetramers were built upon the same batches of streptavidin-PE/allophycocyanin, cooperativity in one and not the other precludes conformational change in streptavidin or the fluorochrome. Furthermore, because of the wide separation between monomeric subunits of tetrameric CD1d1, it is extremely unlikely that a conformational change within CD1d1 itself is responsible for the observed Hill coefficient. This is further emphasized by the fact that CD1d1 dimers made in a manner distinct from tetramers also show cooperative binding. Cooperativity is independent of the parameters of glycolipid binding to CD1d1, because OCH, which interacts with CD1d1 with differing properties than αGalCer, had essentially the same Hill coefficient as αGalCer. Thus, the change in Hill coefficient does not reflect a change in the structure of CD1d1 tetramer, but rather a different organization and/or orientation of the TCR engaging such Ags.

How iNKT cells respond to self-Ag and yet remain quiescent in physiological situations remains unclear. In this study, we demonstrate that iNKT cell receptors exhibit cooperative engagement of glycolipid Ag. Cooperativity in biological systems is a common mechanism for achieving sensitivity to relatively modest changes in the strength of the signal (33, 63). In other words, a relatively small change in ligand concentration will result in full binding/activation of an enzyme/receptor. It is possible that iNKT cells use cooperativity to induce sensitive response to a small change in the concentration of self-Ag. In support of this hypothesis, self-Ag recognition of ex vivo-isolated iNKT cells is dependent on high levels of CD1d1 expression by target cells (2), and conversely, iNKT cell hybridomas recognizing physiologic levels of CD1d1 on target thymocytes or dendritic cells have high levels of Va14Ja18 TCR expression (6). Thus, the finding of cooperativity in iNKT cell Ag engagement, but not among CTL recognizing peptidic Ags may be one mechanism by which iNKT cells recognize self-Ag(s).

Our data indicate that the structure and/or organization of the iNKT cell receptor may be distinct from $\alpha\beta$ TCR of CTL. FG loop within the Cb domain is a large, evolutionarily conserved structure, which forms a wall at the region where Cb and Vb domains of the TCR β-chain join to form a cavity (77). Ab mapping studies revealed that the FG loop is in close proximity to one of the CD3ϵ subunits (78). Transgenic mice expressing the TCR β-chain mutant lacking the FG loop have no gross deficiencies in the development and function of conventional CD4 and CD8 T cells (79), implying that $\alpha\beta$ TCR pairing and surface expression are not grossly impaired. However, a careful analysis in a single specificity TCR transgenic system revealed that thymocytes lacking the FG loop had impaired negative selection (80), but TCR $\alpha\beta$ pairing and expression were unhindered. In contrast, however, Va14Ja18 TCR α-chain was found not to pair at all with a Vb8.2-FG loop mutant, and hence, the mutant mice were impaired in iNKT cell development (81). Interestingly, the anti-TCRβ Ab H57-597, which exhibits strong FRET in conjunction with the CD1d1-αGal-Cer tetramer specifically binds the FG loop (77, 79). However, FRET was not observed in conjunction with H2K^b tetramers or dimers. FRET is observed between CD8a of 2C-transgenic CTL and H2K^b, suggesting the engagement of CD8a by monomeric H2K^b (82). Taken together, the data strongly suggest that the structure and/or the organization of the Va14Ja18 TCR complex are distinct

from $\alpha\beta$ TCR of conventional T cells, which might potentially account for the cooperative engagement of glycolipid Ags.

In conclusion, our findings demonstrate that iNKT cell functions are controlled by narrow avidity thresholds for glycolipid Ags and demonstrate novel properties of their Ag receptor that may have an important role in iNKT cell activation. These findings have important implications for the therapeutic use of iNKT cells.

Acknowledgments

References

1. Joyce, S. 2001. CD1d and natural T cells: how their properties jump start the immune system. *Cell. Mol. Life Sci. 58:442.*
2. Bendelac, A., O. Lantz, M. E. Quimby, J. W. Yewdell, J. R. Bennink, and R. R. Brutkiewicz. 1995. CD1 recognition of mouse NK1$^+$ T lymphocytes. *Science 268:863.*
3. Brossay, L., S. Tangri, M. Bix, S. Cardell, R. Locksley, and M. Kronenberg. 1998. Mouse CD1-autoreactive T cells have diverse patterns of reactivity to CD1$^+$ targets. *J. Immunol. 160:3681.*
4. Chiu, Y. H., J. Jayawardena, A. Weiss, D. Lee, S. H. Park, A. Dautry-Varsat, and A. Bendelac. 1999. Distinct subsets of CD1d-restricted T cells recognize self-antigens loaded in different cellular compartments. *J. Exp. Med. 189:103.*
5. Molano, A., S. H. Park, Y. H. Chiu, S. Nosseir, A. Bendelac, and M. Tsuji. 2000. The IgG response to the circumsporozoite protein is MHC class II-dependent and CD1d-independent: exploring the role of GPIs in NK T cell activation and antimalarial responses. *J. Immunol. 164:5005.*
6. Park, S.-H., J. H. Roark, and A. Bendelac. 1998. Tissue-specific recognition of mouse CD1 molecules. *J. Immunol. 160:3128.*
7. Chiu, Y. H., S. H. Park, K. Benlagha, C. Forestier, J. Jayawardena-Wolf, P. B. Savage, L. Teyton, and A. Bendelac. 2002. Multiple defects in antigen presentation and T cell development by mice expressing cytoplasmic tail-truncated CD1d. *Nat. Immunol. 3:55.*
8. De Silva, A. D., J. J. Park, N. Matsuki, A. K. Stanic, R. R. Brutkiewicz, M. E. Medof, and S. Joyce. 2002. Lipid protein interactions: the assembly of CD1d1 with cellular phospholipids occurs in the endoplasmic reticulum. *J. Immunol. 168:723.*
9. Roberts, T. J., V Sriram, P. M. Spence, M. Gui, K. Hayakawa, I. Bacik, J. R. Bennink, J. W. Yewdell, and R. R. Brutkiewicz. 2002. Recycling CD1d1 molecules present endogenous antigens processed in an endocytic compartment to NKT cells. *J. Immunol. 168:5409.*
10. Brossay, L., M. Chioda, N. Burdin, Y. Koezuka, G. Casorati, P. Dellabona, and M. Kronenberg. 1998. CD1d-mediated recognition of an α-galactosylceramide by natural killer T cells is highly conserved through mammalian evolution. *J. Exp. Med. 188:1521.*
11. Burdin, N., L. Brossay, Y. Koezuka, S. T. Smiley, M. J. Grusby, M. Gui, M. Taniguchi, K. Hayakawa, and M. Kronenberg. 1998. Selective ability of mouse CD1 to present glycolipids α-galactosylceramide specifically stimulates Va14$^+$ NK T lymphocytes. *J. Immunol. 161:3271.*
12. Kawano, T., J. Cui, Y. Koezuka, I. Toura, Y. Kaneko, K. Motoki, H. Ueno, R. Nakagawa, H. Sato, E. Kondo, et al. 1997. CD1d-restricted and TCR-mediated activation of Va14 NKT cells by glycosylceramides. *Science 278:1626.*
13. Nieda, M., A. Nicol, Y. Koezuka, A. Kikuchi, T. Takahashi, H. Nakamura, H. Furukawa, T. Yabe, Y. Ishikawa, K. Tadokoro, and T. Juji. 1999. Activation of human Va24NKT cells by α-glycosylceramide in a CD1d-restricted and Va24TCR-mediated manner. *Hum. Immunol. 60:10.*
14. Spada, F. M., Y. Koezuka, and S. A. Porcelli. 1998. CD1d-restricted recognition of synthetic glycolipid antigens by human natural killer T cells. *J. Exp. Med. 188:1529.*
15. Stanic, A. K., A. D. De Silva, J. J. Park, V. Sriram, S. Ichikawa, Y. Hirabyashi, K. Hayakawa, L. Van Kaer, R. R. Brutkiewicz, and S. Joyce. 2003. Defective presentation of the CD1d1-restricted natural Va14Ja18 NKT lymphocyte antigen caused by β-D-glucosylceramide synthase deficiency. *Proc. Natl. Acad. Sci. USA 100:1849.*
16. Bendelac, A., and R. Medzhitov. 2002. Adjuvants of immunity: harnessing innate immunity to promote adaptive immunity. *J. Exp. Med. 195:F19.*
17. Hong, S., M. T. Wilson, I. Serizawa, L. Wu, N. Singh, O. V Naidenko, T. Miura, T. Haba, D. C. Scherer, J. Wei, et al. 2001. The natural killer T-cell ligand α-galactosylceramide prevents autoimmune diabetes in non-obese diabetic mice. *Nat. Med. 7:1052.*

18. Sharif, S., G. A. Arreaza, P. Zucker, Q. S. Mi, J. Sondhi, O. V. Naidenko, M. Kronenberg, Y. Koezuka, T. L. Delovitch, J. M. Gombert, et al. 2001. Activation of natural killer T cells by α-galactosylceramide treatment prevents the onset and recurrence of autoimmune type 1 diabetes. *Nat. Med. 7:1057*.

19. Miyamoto, K., S. Miyake, and T. Yamamura. 2001. A synthetic glycolipid prevents autoimmune encephalomyelitis by inducing Th2 bias of natural killer T cells. *Nature 413:531*.

20. Singh, A. K., M. T. Wilson, S. Hong, D. Olivares-Villagomez, C. Du, A. K. Stanic, S. Joyce, S. Sriram, Y. Koezuka, and L. Van Kaer. 2001. Natural killer T cell activation protects mice against experimental autoimmune encephalomyelitis. *J. Exp. Med. 194:1801*.

21. Wilson, M. T., A. K. Singh, and L. Van Kaer. 2002. Immunotherapy with ligands of natural killer T cells. *Trends Mol. Med. 8:225*.

22. Margulies, D. H. 1997. Interactions of TCRs with MHC-peptide complexes: a quantitative basis for mechanistic models. *Curr. Opin. Immunol. 9:390*.

23. Davis, M. M., J. J. Boniface, Z. Reich, D. Lyons, J. Hampl, B. Arden, and Y. Chien. 1998. Ligand recognition by αβ T cell receptors. *Annu. Rev. Immunol. 16:523*.

24. Germain, R. N., and I. Stefanova. 1999. The dynamics of T cell receptor signaling: complex orchestration and the key roles of tempo and cooperation. *Annu. Rev. Immunol. 17:467*.

25. Garcia, K. C., L. Teyton, and I. A. Wilson. 1999. Structural basis for T cell recognition. *Annu. Rev. Immunol. 17:369*.

26. Sidobre, S., O. V. Naidenko, B. C. Sim, N. R. Gascoigne, K. C. Garcia, and M. Kronenberg. 2002. The Va14 NKT cell TCR exhibits high-affinity binding to a glycolipid/CD1d complex. *J. Immunol. 169:1340*.

27. Schumann, J., R. B. Voyle, B. Y. Wei, and H. R. MacDonald 2003. Influence of the TCR Vβ domain on the avidity of CD1d α-galactosylceramide binding by invariant Va14 NKT cells. *J. Immunol. 170:5815*.

28. Kalergis, A. M., N. Boucheron, M. A. Doucey, E. Palmieri, E. C. Goyarts, Z. Vegh, I. F. Luescher, and S. G. Nathenson. 2001. Efficient T cell activation requires an optimal dwell-time of interaction between the TCR and the pMHC complex. *Nat. Immunol. 2:229*.

29. Holler, P. D., and D. M. Kranz. 2003. Quantitative analysis of the contribution of TCR:pepMHC affinity and CD8 to T cell activation. *Immunity 18:255*.

30. Garcia K. C., C. A. Scott, A. Brunmark, F. R. Carbone, P. A. Peterson, I. A. Wilson, and L. Teyton. 1996. CD8 enhances formation of stable T-cell receptor/MHC class I molecule complexes. *Nature 384:577*.

31. Luescher, I. F., E. Vivier, A. Layer, J. Mahiou, F. Godeau, B. Malissen, and P. Romero. 1995. CD8 modulation of T-cell antigen receptor-ligand interactions on living cytotoxic T lymphocytes. *Nature 373:353*.

32. Jelonek, M. T., B. J. Classon, P. J. Hudson, and D. H. Margulies. 1998. Direct binding of the MHC class I molecule H-2L^d to CD8: interaction with the amino terminus of a mature cell surface protein. *J. Immunol. 160:2809*.

33. Germain, R. N. 2001. The art of the probable: system control in the adaptive immune system. *Science 293:240*.

34. Fersht, A. 1999. *Structure and Mechanism in Protein Science*. Freeman, New York.

35. Benlagha, K., A. Weiss, A. Beavis, L. Teyton, and A. Bendelac. 2000. In vivo identification of glycolipid antigen-specific T cells using fluorescent CD1d tetramers. *J. Exp. Med. 191:1895*.

36. Cui, J., S Tahiro, T. Kawano, H. Sato, E. Kondo, I. Toura, Y. Kaneko, H. Koseki, M. Kanno, and M. Taniguchi. 1997. Requirement for Va14 NKT cells in IL-12-mediated rejection of tumors. *Science 278:1623*.

37. Mendiratta, S. K., W. D. Martin, S. Hong, A. Boesteanu, S. Joyce, and L. Van Kaer. 1997. CD1d1 mutant mice are deficient in natural T cells that promptly produce IL-4. *Immunity 6:469*.

38. Choi, E. Y., Y. Yoshimura, G. J. Christianson, T. J. Sproule, S. Malarkannan, N. Shastri, S. Joyce, and D. C. Roopenian. 2001. Quantitative analysis of the immune response to mouse non-MHC transplantation antigens in vivo: the H60 histocompatibility antigen dominates over all others. *J. Immunol. 166:4370*.

39. Mylin, L. M., T. D. Schell, D. Roberts, M. Epler, A. Boesteanu, E. J. Collins, J. A. Frelinger, S. Joyce, and S. S. Tevethia. 2000. Quantitation of CD8+ T-lymphocyte responses to multiple epitopes from Simian virus 40 (SV40) large T antigen in C57BL/6 mice immunized with SV40, SV40 T-antigen-transformed cells, or vaccinia virus recombinants expressing full-length T antigen or epitope minigenes. *J. Virol. 74:6922*.

40. Gui, M., J. Li, L. J. Wen, R. R. Hardy, and K. Hayakawa. 2001. TCRβ chain influences but does not solely control autoreactivity of Va14Ja281 T cells. *J. Immunol. 167:6239*.

41. Lantz, O., and A. Bendelac. 1994. An invariant T cell receptor α chain is used by a unique subset of MHC class I specific CD4+ and CD4−8− T cells in mice and humans. *J. Exp. Med. 180:1097*.

42. Limbird, L. E. 1996. *Cell Surface Receptors: A Short Course on Theory and Methods*. Kluwer, Boston.

43. Matsuki, N., A. K. Stanic, M. E. Embers, L. Van Kaer, L. Morel, and S. Joyce. 2003. Genetic dissection of Va14Ja18 natural T cell number and function in autoimmune-prone mice. *J. Immunol. 170:5429*.

44. Joyce, S., A. S. Woods, J. W. Yewdell, J. R. Bennink, A. D. De Silva, A. Boesteanu, S. P. Balk, R. J. Cotter, and R. R. Brutkiewicz 1998. Natural ligand of mouse CD1d1: cellular glycosylphosphatidylinositol. *Science 279:1541*.

45. Boyd, L. F., S. Kozlowski, and D. H. Margulies. 1992. Solution binding of an antigenic peptide to a major histocompatibility complex class I molecule and the role of β2-microglobulin. *Proc. Natl. Acad. Sci. USA 89:2242*.

46. Corr, M., A. E. Slanetz, L. F. Boyd, M. T. Jelonek, S. Khilko, B. K. AlRamadi, Y. S. Kim, S. E. Maher, A. L. M. Bothwell, and D. H. Margulies. 1994. T cell

47. Matsui, K., J. J. Boniface, P. A. Reay, H. Schild, B. Fazekas de St. Groth, and M. M. Davis. 1991. Low affinity interaction of peptide-MHC complexes with T cell receptors. *Science 254:1788*.

48. Crawford, F., H. Kozono, J. White, P. Marrack, and J. Kappler. 1998. Detection of antigen-specific T cells with multivalent soluble class II MHC covalent peptide complexes. *Immunity 8:675*.

49. Savage, P. A., J. J. Boniface, and M. M. Davis. 1999. A kinetic basis for T cell receptor repertoire selection during an immune response. *Immunity 10:485*.

50. Fahmy, T. M., J. G. Bieler, M. Edidin, and J. P. Schneck. 2001. Increased TCR avidity after T cell activation: a mechanism for sensing low-density antigen. *Immunity 14:135*.

51. Rosette, C., G. Werlen, M. A. Daniels, P. O. Holman, S. M. Alam, P. J. Travers, N. R. Gascoigne, E. Palmer, and S. C. Jameson. 2001. The impact of duration versus extent of TCR occupancy on T cell activation: a revision of the kinetic proofreading model. *Immunity 15:59*.

52. Savage, P. A., and M. M. Davis. 2001. A kinetic window constricts the T cell receptor repertoire in the thymus. *Immunity 14:243*.

53. Busch, D. H., and E. G. Pamer. 1999 T cell affinity maturation by selective expansion during infection. *J. Exp. Med. 189:701*.

54. Constant, S., C. Pfeiffer, A. Woodard, T. Pasqualini, and K. Bottomly. 1995. Extent of T cell receptor ligation can determine the functional differentiation of naive CD4+ T cells. *J. Exp. Med. 182:1591*.

55. Hemmer, B., I. Stefanova, M. Vergelli, R. N. Germain, and R. Martin. 1998 Relationships among TCR ligand potency, thresholds for effector function elicitation, and the quality of early signaling events in human T cells. *J. Immunol. 160:5807*.

56. Itoh, Y., and R. N. Germain. 1997. Single cell analysis reveals regulated hierarchical T cell antigen receptor signaling thresholds and intraclonal heterogeneity for individual cytokine responses of CD4+ T cells. *J. Exp. Med. 186:757*.

57. Itoh, Y., B. Hemmer, R. Martin, and R. N. Germain. 1999. Serial TCR engagement and down-modulation by peptide:MHC molecule ligands: relationship to the quality of individual TCR signaling events. *J. Immunol. 162:2073*.

58. Tao, X., S. Constant, P. Jorritsma, and K. Bottomly. 1997. Strength of TCR signal determines the costimulatory requirements for Th1 and Th2 CD4+ T cells differentiation. *J. Immunol. 159:5956*.

59. Carnaud, C., D. Lee, O. Donnars, S.-H. Park, A. Beavis, Y. Koezuka, and A. Bendelac. 1999. Cross-talk between cells of the innate immune system: NKT cells rapidly activate NK cells. *J. Immunol. 163:4647*.

60. Liu, H., M. Rhodes, D. L. Wiest, and D. A. Vignali. 2000. On the dynamics of TCR:CD3 complex cell surface expression and downmodulation. *Immunity 13:665*.

61. San Jose, E., A. Borroto, F. Niedergang, A. Alcover, and B. Alarcon 2000. Triggering the TCR complex causes the downregulation of nonengaged receptors by a signal transduction-dependent mechanism. *Immunity 12:161*.

62. Valitutti, S., S. Muller, M. Salio, and A. Lanzavecchia. 1997. Degradation of T cell receptor (TCR)-CD3-ζ complexes after antigenic stimulation. *J. Exp. Med. 185:1859*.

63. Royer, W. E., Jr., J. E. Knapp, K. Strand, and H. A. Heaslet. 2001. Cooperative hemoglobins: conserved fold, diverse quaternary assemblies and allosteric mechanisms. *Trends Biochem. Sci. 26:297*.

64. Joyce, S., P. Tabaczewski, R. H. Angeletti, S. G. Nathenson, and I. Stroynowski. 1994. A non-polymorphic MHC class Ib molecule binds a large array of diverse self peptides. *J. Exp. Med. 179:579*.

65. Hartel, S., H. A. Diehl, and F. Ojeda. 1998. Methyl-β-cyclodextrins and liposomes as water-soluble carriers for cholesterol incorporation into membranes and its evaluation by a microenzymatic fluorescence assay and membrane fluidity-sensitive dyes. *Anal. Biochem. 258:277*.

66. Brown, D. A., and E. London. 2000. Structure and function of sphingolipid- and cholesterol-rich membrane rafts. *J. Biol. Chem. 275:17221*.

67. Fujii, S., K. Shimizu, M. Kronenberg, and R. M. Steinman. 2002. Prolonged IFN-γ-producing NKT response induced with α-galactosylceramide-loaded DCs. *Nat. Immunol. 3:867*.

68. Leitenberg, D., and K. Bottomly. 1999 Regulation of naive T cell differentiation by varying the potency of TCR signal transduction. *Semin. Immunol. 11:283*.

69. Baxter, A. G., S. J. Kinder, K. J. L. Hammond, R. Scollay, and D. I. Godfrey. 1997. Association between αβTCR+CD4−CD8− T-cell deficiency and IDDM in NOD/Lt mice. *Diabetes 46:572*.

70. Godfrey, D. I., S. J. Kinder, P. Silvera, and A. G. Baxter. 1997 Flow cytometric study of T cell development in NOD mice reveals a deficiency in αβTCR+CDR−CD8− thymocytes. *J. Autoimmun. 10:279*.

71. Hammond, K. J. L., L. D. Poulton, L. Palmisano, P. Silveira, D. I. Godfrey, and A. G. Baxter. 1998 α/β-T cell receptor (TCR)+CD4−CD8− (NKT) thymocytes prevent insulin-dependent diabetes mellitus in non-obese diabetic (NOD)/Lt mice by the influence of interleukin (IL)-4 and/or IL-10. *J. Exp. Med. 187:1047*.

72. Beaudoin, L., V. Laloux, J. Novak, B. Lucas, and A. Lehuen. 2002. NKT cells inhibit the onset of diabetes by impairing the development of pathogenic T cells specific for pancreatic β cells. *Immunity 17:725*.

73. Lehuen, A., O. Lantz, L. Beaudoin, V. Laloux, C. Carnaud, A. Bendelac, J. F. Bach, and R. C. Monteiro. 1998. Overexpression of natural killer T cells protects Va14Ja281 transgenic nonobese diabetic mice against diabetes. *J. Exp. Med. 188:1831*.

74. Naumov, Y. N., K. S. Bahjat, R. Gausling, R. Abraham, M. A. Exley, Y. Koezuka, S. B. Balk, J. L. Strominger, M. Clare-Salzer, and S. B. Wilson. 2001. Activation of CD1d-restricted T cells protects NOD mice from developing diabetes by regulating dendritic cell subsets. *Proc. Natl. Acad. Sci. USA* 98:13838.

75. Chun, T., M. J. Page, L. Gapin, J. L. Matsuda, H. Xu, H. Nguyen, H. S. Kang, A. K. Stanic, S. Joyce, W. A. Koltun, et al. 2003. CD1d-expressing dendritic cells but not thymic epithelial cells can mediate negative selection of NKT Cells. *J. Exp. Med. 197:907.*

76. Call, M. E., J. Pyrdol, M. Wiedmann, and K. W. Wucherpfennig. 2002. The organizing principle in the formation of the T cell receptor-CD3 complex. *Cell 111:967.*

77. Wang, J., K. Lim, A. Smolyar, M. Teng, J. Liu, A. G. Tse, R. E. Hussey, Y. Chishti, C. T. Thomson, R. M. Sweet, et al. 1998. Atomic structure of an αβ T cell receptor (TCR) heterodimer in complex with an anti-TCR Fab fragment derived from a mitogenic antibody. *EMBO J. 17:10.*

78. Ghendler, Y., A. Smolyar, H. C. Chang, and E. L. Reinherz. 1998. One of the CD3ε subunits within a T cell receptor complex lies in close proximity to the Cβ FG loop. *J. Exp. Med. 187:1529*

79. Degermann, S., G. Sollami, and K. Karjalainen. 1999. T cell receptor β chain lacking the large solvent-exposed Cβ FG loop supports normal α/β T cell development and function in transgenic mice. *J. Exp. Med. 189:1679.*

80. Sasada, T., M. Touma, H. C. Chang, L. K. Clayton, J. H. Wang, and E. L. Reinherz. 2002. Involvement of the TCR Cβ FG loop in thymic selection and T cell function. *J. Exp. Med. 195:1419.*

81. Degermann, S., G. Sollami, and K. Karjalainen. 1999. Impaired NK1.1 T cell development in mice transgenic for a T cell receptor β chain lacking the large, solvent-exposed Cβ FG loop. *J. Exp. Med. 190:1357.*

82. Block, M. S., A. J. Johnson, Y. Mendez-Fernandez, and L. R. Pease. 2001. Monomeric class I molecules mediate TCR/CD3ε/CD8 interaction on the surface of T cells. *J. Immunol. 167:821.*

Autoantibodies from primary biliary cirrhosis patients with anti-p95c antibodies bind to recombinant p97/VCP and inhibit *in vitro* nuclear envelope assembly

K. MIYACHI*, Y. HIRANO†, T. HORIGOME†, T. MIMORI‡, H. MIYAKAWA§, Y. ONOZUKA¶, M. SHIBATA**,
M. HIRAKATA††, A. SUWA††, H. HOSAKA‡‡, S. MATSUSHIMA§§, T. KOMATSU§§, H. MATSUSHIMA*, R. W. HANKINS*
& M. J. FRITZLER¶¶ *Health Sciences Research Institute, †Niigata University, Faculty of Science, ‡Kyoto University, §Teikyo
Misonokuchi Hospital, ¶Social Insurance Central Hospital, **East Kanto NTT Hospital, ††Keio University, School of Medicine,
‡‡Yokohama Nanbu Hospital, §§Yokohama Medical Center, National Hospital, Japan, and ¶¶University of Calgary, Faculty of Medicine,
Calgary, Canada

SUMMARY

We have reported previously that p95c, a novel 95-kDa cytosolic protein, was the target of autoanti-
bodies in sera of patients with autoimmune hepatic diseases. We studied 30 sera that were shown pre-
viously to immunoprecipitate a 95 kDa protein from [^{35}S]-methionine-labelled HeLa lysates and had a
specific precipitin band in immunodiffusion. Thirteen sera were available to test the ability of p95c anti-
bodies to inhibit nuclear envelope assembly in an *in vitro* assay in which confocal fluorescence micros-
copy was also used to identify the stages at which nuclear assembly was inhibited. The percentage
inhibition of nuclear envelope assembly of the 13 sera ranged from 7% to 99% and nuclear envelope
assembly and the swelling of nucleus was inhibited at several stages. The percentage inhibition of
nuclear assembly was correlated with the titre of anti-p95c as determined by immunodiffusion. To con-
firm the identity of this autoantigen, we used a full-length cDNA of the p97/valosin-containing protein
(VCP) to produce a radiolabelled recombinant protein that was then used in an immunoprecipitation
(IP) assay. Our study demonstrated that 12 of the 13 (93%) human sera with antibodies to p95c immu-
noprecipitated recombinant p97/VCP. Because p95c and p97 have similar molecular masses and cell
localization, and because the majority of sera bind recombinant p97/VCP and anti-p95c antibodies
inhibit nuclear assembly, this is compelling evidence that p95c and p97/VCP are identical.

Keywords autoantibody conformational epitope nuclear envelope assembly p95c
p97/VCP primary biliary cirrhosis

INTRODUCTION

Patients with autoimmune liver diseases such as primary biliary
cirrhosis (PBC), autoimmune hepatitis (AIH), autoimmune cho-
langiopathy (AIC) and primary sclerosing cholangitis (PSC) pro-
duce autoantibodies that differ from those found in patients with
systemic rheumatic diseases such as rheumatoid arthritis (RA),
systemic lupus erythematosus (SLE), systemic sclerosis (SSc) and
Sjögren's syndrome (SjS) [1–3]. In particular, anti-mitochondrial
antibodies (AMA) have been reported in 85–90% of patients
with PBC and these are among the most prevalent autoantibodies
found in any autoimmune disease [4–6]. Autoantibodies that bind
to components of the nuclear envelope, such as anti-gp210 and
anti-p62 complex, are also important markers for the diagnosis of

PBC patients with and without AMA, and for monitoring the
progression of disease [7–9]. Other studies have shown that
anticentromere antibodies, especially anticentromere B antibody,
anti-SP100 and antibodies to high mobility group (HMG) pro-
teins 1 and 2 may also be useful for the diagnosis of PBC [10–14].
Anti-liver kidney microsome (LKM) antibody and peripheral
antineutrophil cytoplasmic antibodies (p-ANCA) are valuable for
the diagnosis of type 2 AIH [15,16] and PSC [17].

In 1998, we reported a novel antibody directed against a con-
formational epitope on a 95-kDa protein in patients with
autoimmune hepatic diseases [18]. This antibody was found in
12% of PBC and 9·7% of AIH patients, but was not detected in
other autoimmune conditions without hepatic involvement.
Interestingly, unlike LKM and AMA and many other autoanti-
gens, this antigen was not detected by immunoblot. Double
immunodiffusion that used antigens extracted from rat liver
homogenates showed a specific precipitin line that was different
from other known immune precipitin systems [18]. Based on

Correspondence: Kiyomitsu Miyachi MD, Health Sciences Research
Institute, 106 Godo-cho, Hodogaya-ku, Yokohama, Kanagawa, Japan.
  E-mail: mkiyomitsumd_8@hotmail.com

568

immunoprecipitation of extracts of metabolically labelled HeLa cells, the molecular mass of this autoantigen was estimated to be 95 kDa.

Recently, p97/VCP (valosin-containing protein) was characterized and found to play an important role in nuclear envelope assembly and the formation of the endoplasmic reticulum and Golgi apparatus during the final stage of mitosis [19,20]. Of interest, antibodies to p97/VCP inhibited nuclear reassembly *in vitro* [21]. Based on studies and paradigms of other autoantibodies that bind to and inhibit functional domains or active sites of the cognate antigens [2], we reasoned that if autoantibodies to p95 and p97/VCP were identical that they too would reduce its biological activity and inhibit nuclear assembly. In this study, we have sought to determine whether the cognate antigen of anti-p95c and p97/VCP are identical by investigating the ability of the autoantibody to inhibit nuclear envelope assembly and to immunoprecipitate recombinant p97/VCP.

MATERIALS AND METHODS

Patients and sera

Thirty sera with antibodies to p95c were identified by immunodiffusion in a serum bank established in the Health Sciences Research Institute. The diagnosis of the patients was established according to published clinical parameters and histological features of liver biopsies [22,23]. Sufficient amounts of sera from 13 patients were available for the inhibition of nuclear envelope assembly assay and to identify anti-p95c to anti-p97/VCP by immunoprecipitation (described below). A prototype serum (I) with antibodies to p95c and normal human serum were used as controls to study the steps of nuclear assembly inhibition during the cell cycle by confocal immunofluorescence microscopy.

Indirect immunofluorescence

Antinuclear antibody (ANA) and AMA were detected by indirect immunofluorescence, as described in detail elsewhere [24]. Briefly, HEp-2 slides and cryostat sectioned rat kidney and stomach (Fluoro AID 1 test, MBL Inc., Japan) were used for ANA and AMA, respectively. The sera were incubated on the substrates and after excess antibody was washed away and they were then incubated with polyvalent anti-human immunoglobulin conjugated to fluorescein isothiocyanate. The slides were read on a fluorescence microscope (Nippon Optico, Japan).

Double immunodiffusion

The Ouchterlony double immunodiffusion (ID) method was used to demonstrate the identity of precipitin reactions between soluble antigen and serum antibodies. The antigen source was prepared from rat liver mitochondrial, microsomal and supernatant fractions as described previously [18]. The mitochondrial fraction was sonicated (Tosho Electric Company, Japan) for 45 s at full power to release antigens and the protein concentration of the soluble antigens determined as described previously [18]. Sixty mg/ml of the microsomal fraction was then used as the antigen source for the detection of anti-LKM 1 and anti-p95c antibodies. Conventional antimitochondrial antibodies (i.e. antibodies to pyruvate dehydrogenase complex) and antibodies to nuclear antigens, such as anti-U1RNP, Sjögren's syndrome antigen A (SS-A)/

Ro and anti-Sm, were not detected under these experimental conditions [25].

In vitro transcription/translation and immunoprecipitation

The cDNA representing the full-length valosin-containing protein (p97/VCP: Accession number CAA78412; a gift from Dr Graham Warren, Yale University, New Haven, CT, USA) was used as a template for *in vitro* transcription and translation (TnT, Promega, Madison, WI, USA) in the presence of [^{35}S]-methionine as described previously [26,27]. TnT reactions were conducted at 30°C for 1·5–2 h and the presence of translation products was confirmed by subjecting 2–5 μl samples to sodium dodecyl sulphate–polyacrylamide gel electrophoresis (SDS-PAGE) and analysis by autoradiography. The *in vitro* translated products were then used as the antigen source. IP reactions were prepared by combining 100 μl 10% protein A-Sepharose beads (Sigma, catalogue no. P-3391), 10 μl human serum, 500 μl NET2 buffer (50 mM Tris-HCl, pH 7·4, 150 mM NaCl, 5 mM EDTA, 0·5% Nonidet P-40, 0·5% deoxycholic acid, 0·1% SDS, 0·02% sodium azide) and 5–10 μl of labelled recombinant protein obtained from the TnT reaction described above. After 1 h of incubation at 4–8°C, the Sepharose beads were washed five times in NET2, and the proteins eluted in 10 μl of sample buffer. The proteins were analysed by 10% or 12·5% SDS-PAGE as described previously [26].

Nuclear assembly assays

Demembranated sperm chromatin was prepared as described [28] and stored at −80°C at a concentration of 40 000 units/μl. *Xenopus* sp. eggs were collected, the jelly layer removed and then lysed to prepare an interphase extract [29]. The nuclear envelope assembly assays were then performed essentially as described by Smythe and Newport [30]. Briefly, the *Xenopus* egg extracts, cytosol and membrane fractions were supplemented with an ATP regenerating system (10 mM phosphocreatine, 2 mM ATP (pH 7·0), 5 μg/ml creatine kinase), and then mixed with demembranated sperm chromatin. The standard reaction mixture consisted of 10 000 units of chromatin and 10 μl crude extract or 10 μl cytosol + 1 μl membrane. After incubation at room temperature (23°C) for 1·5 h, a 2 μl aliquot of the reaction mixture was removed and diluted with 2 μl of Hoechst in dihexylocarbocyanine iodine (DHCC) buffer (15 mM PIPES-KOH, pH 7·4, 0·2 M sucrose, 7 mM MgCl$_2$, 80 mM KCl, 15 mM NaCl, 5 mM EDTA) containing 20 mg/ml bis-benzimide DNA dye (Hoechst 33342; Calbiochem-Novabichem), a lipid dye, 3,3'-DHCC (Aldrich, Japan), and 3·7% formaldehyde on a glass slide. The sample was mounted with a cover-slip and examined under a 100x objective lens on a phase contrast and Axioplan fluorescence microscope (Carl Zeiss) fitted with exciter barrier reflector combinations appropriate for the fluorescent dyes described above.

For confocal microscopy, DNA was visualized by staining the preparations with propidium iodide and DHCC. Images were recorded with a Radiance 2000 confocal fluorescence system (Bio-Rad, Tokyo) mounted on a Nikon E600 fluorescence microscope (Nikon, Tokyo). The rate of inhibition of nuclear assembly was calculated by applying the formula: corrected inhibition rate of nuclear assembly (%) = (inhibition rate of nuclear assembly obtained from adding patient's serum (%) − inhibition rate of nuclear assembly obtained from adding normal healthy serum (%)/nuclear assembly obtained from adding normal healthy serum (%)

RESULTS

The diagnosis of the 30 patients that IP the p95c protein included 23 with PBC and seven with AIH (Table 1). Twenty-four of the 30 (80%) patients were female. Twelve patients presented with other concurrent diseases: eight with SjS, two with Hashimoto's thyroiditis, one with RA and one with dilated cardiomyopathy. Within the group of eight SjS patients, four had an overlap syndrome manifested as SLE/SjS, SSc/SjS, mixed connective tissue disease (MCTD)/SjS or RA/SjS. Among the 13 PBC patients that had a liver biopsy, two cases were classified as Scheuer stage 4, but the remaining cases were classified as either stage 1 or 2.

Antimitochondrial antibodies (AMA) were detected in 21 (70%) of the sera with titres ranging from 1/20 to 1/640. A positive ANA was observed in 18 patients with titres that ranged from 1/40 to 1/20 480. Eight patients had antibodies to SS-A, 5 had anti-U1RNP and one with a PBC/SjS/SSc overlap syndrome had antitopoisomerase 1.

Inhibition of in vitro nuclear envelope assembly

The 13 sera (PBC 10, AIH 3) with p95c antibodies demonstrated 7–99% inhibition of the envelope assembly in the *in vitro* assay (Table 1). When the data are plotted as percentage of inhibition rates (Fig. 1), the degree of inhibition was correlated with the titre of anti-p95c. In separate experiments, crude *Xenopus* egg extracts were pre-incubated with buffer alone, control normal serum and a prototype serum (IK). The degree and stage at which nuclear assembly was inhibited was examined by adding *Xenopus* sperm chromatin to the reaction. Pre-incubation with buffer or normal serum yielded continuous nuclear rim-staining with the phospholipid stain DHCC, indicating the presence of assembled chromatin (Fig. 2). On the other hand, pre-incubation with the prototype serum yielded discontinuous lipid-staining of the nuclear rims with some areas well covered by membrane while others were not (Fig. 2). When the surface of the chromatin was viewed under higher magnification, the nuclear envelope was not fully enclosed and the lipid-staining was reticulated.

Table 1. Clinical and serological features of 30 patients with antibodies to p95c

No.	Sex	Liver biopsy	Primary diagnosis*	Secondary diagnosis	AMA titre**	ANA titre**	ANA specificity	Anti-p95c ID**	Anti-VCP IP	INA %
1	M	+	PBC:S1-2	SjS	160	160	U1RNP/SS-A	128	+ +	82
2	F	n.d.	AIH	SjS	–	80	U1RNP/SS-A	1	+ + +	67
3	F	n.d.	AIH	SLE/SjS	–	640	U1RNP/SS-A	8	+ +	29
4	F	n.a.	PBC	–	40	–	–	32	+ + +	13
5	F	n.a.	PBC	–	–	–	–	1024	+ + + +	88
6	M	+	PBC:S1	–	40	80	–	256	+ + + +	59
7	M	n.d.	PBC	–	40	–	–	64	+ + + +	64
8	F	n.d.	PBC	–	–	40	–	16	+ + +	13
9	F	+	AIH	–	–	–	–	16	+	7
10	F	+	PBC:S2	–	40	–	–	64	–/+	99
11	F	+	PBC:S1	Hashimoto	320	80	–	4	+	15
12	F	+	PBC:S1	SjS	80	20	SS-A	32	+ +	23
13	F	n.d.	PBC	–	640	–	–	512	+ + + +	83
14	M	+	PBC:S1	–	80	–	–	16	n.d.	n.d.
15	F	+	PBC:S1	–	160	–	–	256	n.d.	n.d.
16	F	+	PBC:S2	–	160	320	–	2	n.d.	n.d.
17	F	+	PBC:S2	–	320	–	–	16	n.d.	n.d.
18	F	+	PBC:S4	–	640	20	–	16	n.d.	n.d.
19	M	+	PBC:S4	–	640	–	–	8	n.d.	n.d.
20	F	n.d.	PBC	–	160	80	–	32	n.d.	n.d.
21	F	n.d.	PBC	–	640	–	–	128	n.d.	n.d.
22	F	n.d.	PBC	–	320	–	–	32	n.d.	n.d.
23	F	+	PBC:S1	Hashimoto	320	80	–	128	n.d.	n.d.
24	F	+	PBC:S1	SjS/SSc	20	320	SS-A/Topo1	32	n.d.	n.d.
25	F	n.d.	PBC	SjS/MCTD	–	20480	U1RNP/SS-A	16	n.d.	n.d.
26	M	n.d.	PBC	DCM	320	–	–	32	n.d.	n.d.
27	F	+	AIH	–	–	160	–	256	n.d.	n.d.
28	F	+	AIH	SjS	320	320	U1RNP/SS-A	8	n.d.	n.d.
29	F	n.d.	AIH	RA	–	160	–	64	n.d.	n.d.
30	F	n.d.	AIH	SjS/RA	–	160	SS-A	64	n.d.	n.d.

*S indicates Scheuer's staging of liver pathology [22,23]. **AMA, ANA and p95c titres are the reciprocal of number shown; + indicates the semiquantitative reaction with recombinant VCP as determined by the autoradiogram of immunoprecipitated [35S]-labelled protein. AIH, autoimmune hepatitis; AMA, antimitochondrial antibodies; ANA, antinuclear antibodies; DCM, dilated cardiomyopathy; ID, immunodiffusion; INA, inhibition of nuclear assembly; IP, immunoprecipitation: MCTD, mixed connective tissue disease; n.a., result not available; n.d., not done; PBC, primary biliary cirrhosis; RA, rheumatoid arthritis; SjS, Sjögren's syndrome; SLE, systemic lupus erythematosus; SS-A, Sjögren's syndrome antigen A; Topo1, topoisomerase 1; U1RNP, U1 ribonucleoprotein; VCP, valosin-containing protein.

Immunoprecipitation of recombinant p97/VCP

The same 13 sera were then used in an IP assay that employed radiolabelled recombinant p97/VCP produced in the rabbit reticulocyte lysate system (Table 1). Twelve (93%) of the sera immunoprecipitated the ~97 kDa recombinant protein, but normal human sera and PBC sera with antimitochondrial antibodies, but no antibodies to p95c, did not (Fig. 3). One serum (no. 10: Table 1, Fig. 3) showed an equivocal IP result.

DISCUSSION

This study provides compelling evidence that the previously described p95c autoantigen and p97/VCP are the same proteins. This conclusion is based on a number of remarkable similarities between p95c and p97/VCP. First, the molecular masses and cellular localization in the cytosol are nearly identical. Secondly, all sera with anti-p95c antibodies have been shown to inhibit nuclear envelope assembly. Thirdly, all but one of the available 13 sera that had anti-p95 antibodies and inhibited nuclear assembly immunoprecipitated the recombinant p97/VCP protein.

We have shown previously that anti-p95c antibodies that were found in the sera of patients with PBC and AIH were demonstrated easily by immunodiffusion and immunoprecipitation but
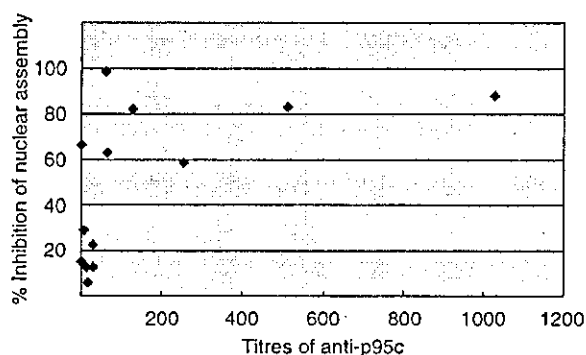

Fig. 1. Relationship between percentage inhibition of nuclear assembly and titres of anti-p95c antibodies in the sera of PBC patients. Sera with low titre (<1 : 128) anti-p95c antibodies exhibit less inhibition of nuclear assembly whereas sera with high titres (>1/128) show the most marked inhibition of nuclear assembly.

could not be detected by conventional immunoblotting techniques [18]. This is in contrast to most autoantibodies found in other autoimmune diseases that usually show reactivity to the cognate antigens by immunoblotting [3,31]. Based on these observations, we suggested that the epitope of the p95c autoantigen was conformational [18].

In the present study, all but one of the sera with anti-p95 antibodies bound to the recombinant p97/VCP protein in an IP assay. In this assay, certain conformational epitopes are probably present, although it is likely that post-translational modifications, which are features of the native protein, are not represented fully in the recombinant protein produced in the rabbit reticulocyte lysate system. The requirement for certain post-translational modifications may explain why the one serum did not immunoprecipitate the recombinant VCP. To gain further insight, studies are under way to map the linear and conformational epitopes on p97/VCP.

When we considered possible autoantigenic targets of the anti-p95c sera, two novel antigens in the cytosol with molecular masses each of 97 kDa came to our attention. The first was β-karyopherin (importin-β), which plays a key role in nuclear import [16]. The other was p97/VCP, which plays an important role in various membrane fusions such as Golgi and nuclear envelope assembly, and ubiquitin-dependent protein degradation [32,33]. This protein is a member of a family of AAA-ATPases, some of which (i.e. F_0-ATPase) are located in the inner mitochondrial membrane [17] and others (i.e. F_1-ATPase) localized to the matrix space [34,35]. The p97/VCP complex and N-ethylmaleimide sensitive fusion protein (NSF) share certain similarities in that they both form ring-shaped homo-hexamers (in contrast to hetero-hexamers of F_1-ATPase) and are involved in biogenesis and functional activities of the Golgi and nuclear membranes [33,36]. The function of p97 can be inhibited by α-SNAP, a component of the NSF pathway, and the function of NSF can be inhibited by p47, also a component of the p97 pathway [32]. The mechanism of nuclear inhibition is thought to involve competition between α-SNAP and p47 to bind syntaxin 5, a common component of the functional p97 and NSF pathways [32].

In our study the inhibition of nuclear assembly was generally correlated with the titre of anti-p95c antibody as determined by ID, but there was a less clear-cut correlation between the nuclear inhibition assay and the semiquantitative assessment of the TnT IP results (Table 1). Therefore, it has yet to be shown conclusively that anti-p95c antibodies are indeed the factors that inhibit the
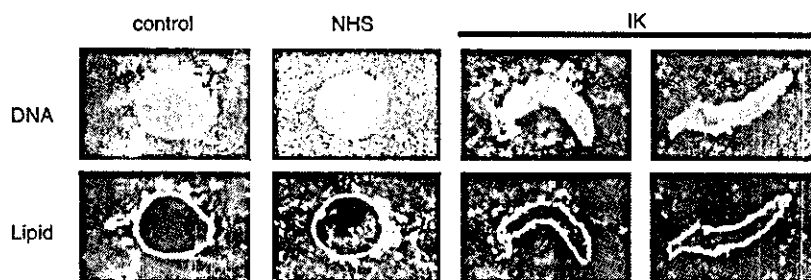

Fig. 2. Confocal immunofluorescent microscopy of the nuclear reassembly assay. Nuclear envelope assembly was inhibited by the index serum (IK) but not by phosphate buffered saline or normal healthy serum. Nuclear assembly was judged to have occurred when the length of the long axis divided by the short axis was less than 2.
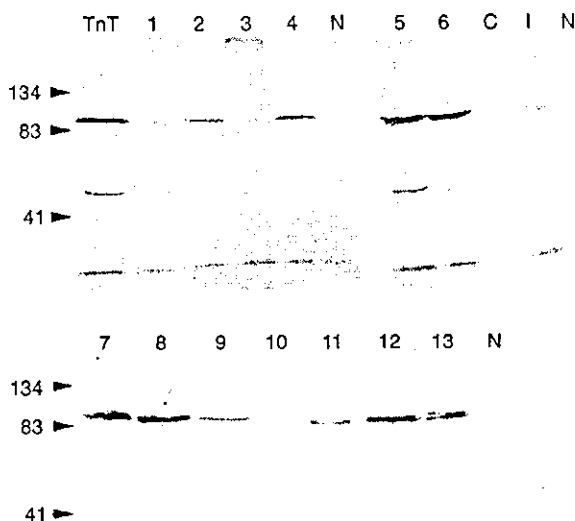
Fig. 3. Immunoprecipitation of p97/VCP recombinant protein with human anti-p95 sera. The p97/VCP protein was expressed as a [^{35}S]-labelled *in vitro* transcription and translation (TnT) product and then immunoprecipitated with the human sera. Thirteen sera with anti-p95c antibodies (lanes 1–13) and the index anti-p95c sera (I) immunoprecipitated the ~97 kDa recombinant protein whereas normal human serum (N) and a control serum from a patient with antimitochondrial antibodies (C) did not. The reactivity of the serum in lane 10 is weak compared to other sera but was equivocally positive on the original imaging film. Molecular weight markers are indicated on the left.

nuclear assembly. A number of observations support our conclusion. First, like our observations, Hetzer and his colleagues demonstrated that anti-p97/VCP antibody inhibits nuclear envelope assembly in a *Xenopus* egg extract in the *in vitro* system [21]. Secondly, we have shown previously that AMA and anti-gp210 antibodies, which are found in sera from patients with PBC [5], and anti-U1RNP/Sm, anti-SS-A/Ro, anti-SS-B/La, which are found in sera from patients with SLE or SjS [2,3], did not inhibit nuclear assembly in the *in vitro* assay (data not shown). However, it remains to be determined if autoimmune sera with antibodies directed against nuclear envelope proteins such as lamin B receptor (LBR), LAP2 (lamina associated polypeptide 2), lamin A/C and lamin B might inhibit nuclear assembly. According to a recent report, some human sera might contain antibodies to other antigens, such as glyceraldehydes-3-phosphate, that also participate in nuclear assembly [28].

Hetzer *et al.* has reported that several steps are involved in the process of nuclear assembly and, specifically, p97–p47 is required for nuclear envelope expansion in the final steps of nuclear envelope fusion [21]. In our study, confocal immunofluorescence microscopy showed that inhibition of nuclear assembly occurred at more than one stage because some areas of chromatin were well covered by the nuclear envelope while others were not. Thus, anti-p95c antibodies may be directed against domains of p97 that are critical in different steps of nuclear envelope assembly. The

antigenic domain(s) bound by anti-p95c is not known; studies are under way to define the primary conformational and linear epitopes. The assumption that human anti-p95c antibodies bind to the active site of p95/VCP and inhibit its function is based on studies of other human autoantibodies that have been shown to bind functional sites of proteins and inhibit their biological activities [37,38].

In summary, we provide evidence that the previously described p95c autoantigen and p97/VCP are identical proteins. To maintain understanding between disciplines we propose that anti-p95c antibodies be referred to as anti-p97/VCP in the future. Anti-p97/VCP was found in approximately 12·5% of patients with PBC and in 9·7% with AIH [18]. In contrast to the prevalence of AMA [5], the prevalence of anti-p95c antibody in PBC is relatively low. Therefore, the diagnostic importance of anti-p95c antibody occurs frequently in AMA-negative PBC and in ANA-negative AIH. In our study, many of the PBC or AIH patients with this antibody had overlap conditions, particularly SjS. Prospective studies of SjS patients would be important to determine if anti-p97/VCP antibodies antedate the appearance of autoimmune liver disease.

ACKNOWLEDGEMENTS

REFERENCES

1 Gershwin ME, Mackay IR, Sturgess A, Coppel RL. Identification and specificity of a cDNA encoding the 70 KD mitochondrial antigen recognized in primary biliary cirrhosis. J Immunol 1987; **138**: 3525–31.

2 Tan EM. Antinuclear antibodies: diagnostic markers for autoimmune diseases and probes for cell biology. Adv Immunol 1989; **44**:93–151.

3 von Muhlen CA, Tan EM. Autoantibodies in the diagnosis of systemic rheumatic disease. Semin Arthritis Rheum 1995; **24**:323–58.

4 Mackay IR. Autoimmunity and primary biliary cirrhosis. Baillières Clin Gastroenterol 2000; **14**:519–33.

5 Fritzler MJ, Manns MP. Anti-mitochondrial antibodies. Clin Appl Immunol Rev 2002; **3**:87–113.

6 Strassburg CP, Obermayer-Straub P, Manns MP. Autoimmunity in liver diseases. Clin Rev Allergy Immunol 2000; **18**:127–39.

7 Courvalin J-C, Worman HJ. Nuclear envelope protein autoantibodies in primary biliary cirrhosis. Semin Liver Dis 1997; **17**:79–90.

8 Miyachi K, Shibata M, Onozuka Y, Kikuchi F, Imai N, Horigome T. Primary biliary cirrhosis sera recognize not only gp210 but also proteins of the p62 complex bearing N-acetyl glucosamine residues from rat liver nuclear envelope. Anti-p62 complex antibody in PBC. Mol Biol Rep 1996; **23**:227–34.

9 Miyachi K, Hankins RW, Matsushima H *et al.* Profile and clinical significance of anti-nuclear envelope antibodies found in patients with primary biliary cirrhosis: a multicenter study. J Autoimmun 2003; **20**:247–54.

10 Makinen D, Fritzler MJ, Davis P, Sherlock S. Anticentromere antibodies in primary biliary cirrhosis. Arthritis Rheum 1983; **26**:914–7.